DESIGN AND SYNTHESIS OF ZN(II)-SALOPHEN DERIVATIVES: FROM CHEMOSENSING TO CATALYSIS

Martina Piccinno

Doctoral Thesis

Università La Sapienza & ICIQ – Institut Català d'Investigació Química

Design and synthesis of Zn(II)-salophen derivatives: from chemosensing to catalysis

Martina Piccinno

Supervisors:
Prof. Antonella Dalla Cort
and Prof. Pablo Ballester

Coordinator:
Prof. Osvaldo Lanzalunga

2015

Prof. Pablo Ballester, ICREA Research Professor & ICIQ Group Leader

Prof. Antonella Dalla Cort, Università La Sapienza Professor

I STATE that the present study, entitled “Design and synthesis of Zn(II)-salophen derivatives: from chemosensing to catalysis”, presented by Martina Piccinno for the award of the degree of Doctor, has been carried out under my supervision at the Institut Català d'Investigació Química (ICIQ) and at the Department of Chemistry of of Università La Sapienza.

Rome, October 13, 2015

Doctoral Thesis Supervisors

Prof. Pablo Ballester

Prof. Antonella Dalla Cort

Acknowledgements

Acknowledgements

First of all I would like to thank my two supervisors: Antonella and Pau. They thought me a lot, both as a chemist and as a person. I will always be grateful to Antonella for teaching me to think wider and proposing me exciting projects. I feel really lucky to having met Pau and have spent in his laboratory a wonderful period, half of my PhD. From him I could learn that being a scientist means not only do experiments but also to understand, explain and write.

I would like to thank Beatriz for her precious help and all the technicians of the ICIQ support units that really helped me a lot during my studies.

Also, I would like to thank they research groups for sharing this period with me. In particular, special thanks go to Gemma, Albano and Ramon. Gemma, gracias por ser siempre disponible ad ayudarme para cualquier cosa, hiciste más de tu trabajo! Gracias a Albano y Ramón por ser amigos y no solo compañeros de trabajo.

Vorrei ringraziare le mie meravigliose amiche, Federica, Gloria e Roberta, che è stato come averle sempre accanto, anche se lontane.

Grazie a mia sorella Camilla, per i suoi piccoli dolci gesti quotidiani.

Un grazie dal profondo del mio cuore va ai miei genitori, che mi hanno sempre incoraggiato, stimato e sostenuto durante tutto il mio percorso di studi.

Infine un grazie speciale va a Mattia, per aver sempre creduto in me e per aver reso il periodo a Tarragona ancora più bello.

Ai miei genitori e Mattia

Table of contents

Chapter 1

General introduction

1.1 Supramolecular chemistry

Supramolecular chemistry was defined by Jean-Marie Lehn as "the chemistry beyond the molecule". It relies on the formation of intermolecular non-covalent bonds between two or more chemical species.[1,2,3,4] The host-guest system formed by a receptor (host) and the substrate (guest) bound, through non-covalent interactions (*i.e.* electrostatic interactions, hydrogen bonding, Van der Waals forces, etc.) is a supermolecule (Figure 1).

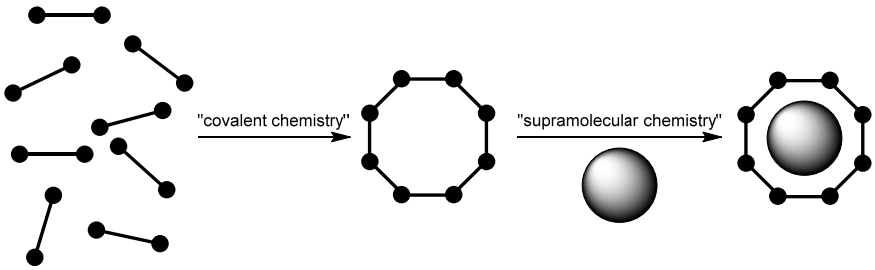

Figure 1. Schematic representation for the covalent and the supramolecular chemistry.

The receptor-substrate interaction can be considered a recognition event that requires shape and size complementarity between the two partners. To obtain specificity in the recognition of a substrate a high degree of synthetic design is required for the receptor. In this Nature is the major source of inspiration for supramolecular chemists. Highly specific molecular interactions such as those taking place between proteins, in enzyme-substrate complexes or between the two helix of the DNA are responsible for the efficiency of all the processes occurring in biology. Supramolecular chemistry is a wide area as demonstrated by the pioneering works by J. M. Lehn and coworkers in the 90's[1] that is increasingly spreading nowadays and includes not only molecular recognition processes, but also the development of functional devices such as molecular machines[5], and plays a fundamental role in many fields like catalysis[6], photochemistry[7], self-replication[8], etc.

1.2 Metal sal(oph)en complexes

Metal-sal(oph)en complexes are a popular class of compounds in supramolecular chemistry. They can be obtained from the condensation reaction of a salicylaldehyde and a diamine in the presence of a metal salt (Scheme 1)[9].

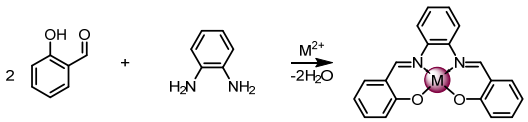

Scheme 1. General scheme for the synthesis of a metal-salophen complex.

The amine can be aliphatic or aromatic, giving rise to the distinction between salen (for the former) and salophen (for the latter). They are tetradentated Shiff-bases with the N_2O_2 atoms belonging to the ligand lying in the same plane. The metal is well positioned in this plane, with the phenolic oxygens and the imine nitrogens participating to metal binding through covalent and coordinative bonds, respectively. Their properties are strictly connected to the nature of the metal, and in particular to its coordination geometry. These features recall porphyrins, but in this case the accessibility to huge amount of compounds is much greater. The possibility to functionalize both the diamine and the salicylaldehyde together with the ease of their preparation render them excellent candidates for the preparation of libraries of compounds.[9,10,11] When the diamine is the *trans*-1,2-diaminocyclohexane the resultant salen is chiral and can be used as chiral catalyst (Figure 2). They became popular in 1990 when Jacobsen and Katsuki described Manganese-salen derivatives as catalysts in the enantioselective epoxidation of unfunctionalized olefins.[12,13]

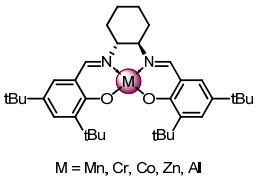

Figure 2. Structure of the metal-salen derivative used as catalyst in many asymmetric reactions.

Later on, salen derivatives of different transition metals were exploited in many other asymmetric reactions such as ring-opening (ARO) of epoxides,[14,15,16] addition of cyanide to imines (Strecker reaction),[17] addition of terminal alkynes to ketones,[18] Henry Reaction,[19] and asymmetric [2+2] cyclocondensation of acyl halides with aliphatic aldehydes.[20]

As mentioned above, chiral salen ligands have received much attention in asymmetric catalysis. However, when one of the building units is *o*-phenylendiamine, extended conjugated π-system are available (Scheme 1). In this kind of systems the π-conjugation imparts a rigid geometry around the metal center, and its Lewis acid character can be easily modulated. Also, new photophysical properties arose that render them excellent candidates as chemosensors. The application of such systems in catalysis is less widespread but some important contributions have to be mentioned.[21]

The group of Mandolini investigated the application of uranyl salophens in catalysis. They found that uranyl complexes catalyzed the 1,4-thiol addition to enones.[22,23] When an aromatic side arm on the salophen structure was present, the molecule was able to stabilize the transition state of a Diels-Alder reaction (Figure 3).[24] Notably, nor the quinone reactant or the reaction product were bound by the catalyst **1**. The uranyl center behaved as a Lewis acid and bound one of the benzoquinone oxygens whose Lewis basicity increased during the reaction. The same reaction was not catalyzed by model compound **2** lacking

the aromatic sidearm, indicating the existence of weak interactions with the sidearm of **1** during the catalysis.

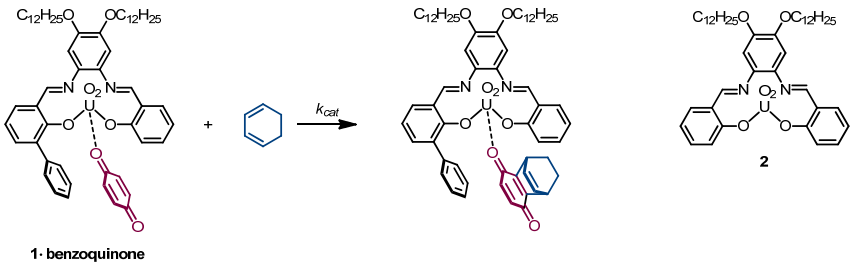

Figure 3. Diels-Alder reaction between benzoquinone and 1,3-cyclohexadiene catalyzed by uranyl-salophen.

Vecchio and co-workers reported the synthesis and spectroscopic characterization of a Mn(III)-salophen complex conjugated with a β-cyclodextrin. The biological activity of the complex was evaluated and superoxide dismutase (SOD)-like activity was determined. It resulted that the presence of the cyclodextrin not only increased water solubility, but also imparted a slight increase to the antioxidant activity of SOD.[25] The same group also described the non-covalent conjugation of a Mn(III)-salophen with bovine serum albumin to prepare an artificial SOD enzyme. According to the authors, the protein has a positive effect and the adduct showed increased SOD activity.[26]

Dimeric Cr(III)-salophen **3** connected through a flexible linker was exploited as bifunctional catalyst in the ring-opening polymerization (ROP) of β-butyrolactone and CO_2/propylene oxide (PO) copolymerization (Figure 4). The dimeric complex **3** gave 5 times higher yield and higher molecular weight of the polymeric product compared with the monomeric one.[27]

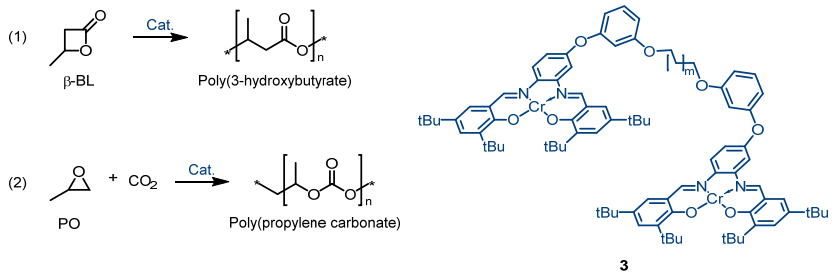

Figure 4. Bifunctional catalyst for the ring-opening polymerization (ROP) of β-butyrolactone (1) and CO2/propylene oxide (PO) copolymerization (2).

1.3 Zinc salophen

An extensive work involving salophen implied their application as ligands in the formation of zinc complexes. Zinc is an essential metal in the biological world, being the second most abundant transition metal in organisms. It is the only metal present in all six enzyme classes. In solution, zinc exists in the +2 oxidation state and has pronounced Lewis acid character because of its small radius to charge ratio. For this reason it can form strong covalent bonds with S, N and O donors.[28] These unique properties of the zinc metal were exploited in Zn(II)-salophen complexes, that found application in many different fields spreading from anion sensor, catalysis, and material chemistry. Below are reported some representative examples regarding the use of Zn(II)-salophen complexes.

1.3.1 Zinc salophen in the formation of supramolecular assemblies

The high Lewis acidity of the zinc metal center in Zn(II)-salophen complexes, together with their strong absorption band in the region of 300-500 nm (depending on the substitution on the salophen ligand) render them excellent candidates as chemosensors. In 2007 Dalla Cort *et al.* studied the ability of some Zn(II)-salophen complexes to bind tertiary amines. They could find that the

binding of a series of tertiary amines was dominated by steric effects. With quinuclidine, for which the steric hindrance around the N atom is minimal, the authors could estimate a binding constant higher than 10^6 M^{-1} in chloroform.[29]

The binding of N donor to Zn(II)-salophen was also exploited by Kleij for the absorption/desorption of alkaloids. They studied the binding event for different alkaloids guests through UV-vis, NMR and X-Ray techniques and measured a binding constant (K_a) for this assemblies in the order of 10^5.[30] When the titration was carried out in a relatively acidic solvent such as chloroform demetalation of Zn(II)-salophen occurred through the activation of a water molecule by a nearby Zn(II)-salophen. However, in the presence of suitable N-donor ligands such as alkaloids, Zn^{2+} could be reincorporated in the salophen backbone. Interestingly, this event gave rise to a color response.[31]

Zinc salophens has also a high affinity for O-anions, such as phosphates and acetates. This tendency allowed Dalla Cort and co-workers to design a receptor for biologically relevant anions such as AMP, ADP and ATP. This receptor featured an extended aromatic wall on the diamine linker that can serve as a second binding site through π-π stacking interactions. The best result could be obtained with ADP where the distance between the phosphate group and the adenine matched the one between Zn^{2+} and the naphtalene ring in the salophen skeleton.[32] The same research group reported a water soluble version of zinc salophen complexes that was able to bind carboxylate anions in water and more interestingly α-aminoacids are detected with a slight degree of enantioselectivity in all cases, with the exception of phenylalanine for which the discrimination between the two enantiomers is much higher. This finding was explicated by the authors as due to a multiple interaction that is zinc-carboxylate coordination and hydrogen bonding between the ammonium group of the aminoacid and two oxygen atoms of one D-glucose moiety, and in

the case of phenylalanine a preferential π-π interaction between one of the enantiomers and the aromatic rings of the salophen ligand.[33]

As reported by Kleij, various anions are bound by the zinc metal center of salophens, giving rise to 1:1 complexes. However, in the case of acetate the situation is slightly different. At low concentration of AcO^- guest, the 2:1 complex is preferentially formed. Beyond 0.5 equivalents of AcO^-, the equilibrium is shifted toward the formation of the 1:1 complex (Figure 5).[34]

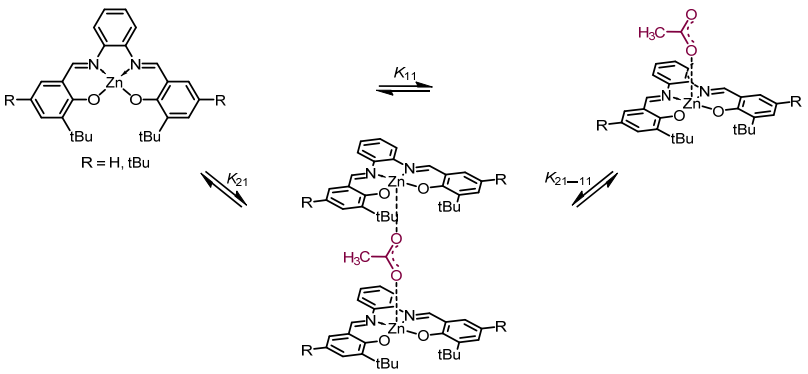

Figure 5. The different equilibria involved in the binding of acetate anion to the Zn(II)-salophen.

1.3.2 Photophysics of Zinc-salophen complexes

Zinc salophen complexes are known to be moderately fluorescent. Hupp and co-workers described the photophysical properties of supramolecular boxes constituted of four Zn(II)-salen (or salophen) held together by rhenium complexes at the edges. The inclusion of another Zn(II)-salen (or salophen) in the box allowed the formation of a pentakis(salen) assembly in which the guest inside and the host square underwent energy transfer.[35]

In 2007, Knapp, described the fluorescence quenching of a Zn(II)-salophen by nitroaromatics. Based on the measurement of the redox potentials the authors proposed a phothoinduced electron-transfer from the excited state of the salophen complex to the nitro compound as responsible for the quenching.[36]

Recently, we described the quenching of the emission of the 1,8-naphthalimide by a Zn(II)-salophen complex (See Chapter 2). The quenching occurred both in the covalently linked and in the supramolecular assembly and was ascribed to a photoinduced energy transfer. Interestingly, the supramolecular, non-fluorescent 1:1 complex constituted of a pyridyl derivative of the 1,8-naphthalimide and a Zn(II)-salophen complex was exploited as an on-off-on anion receptor according to the fluorescent displacement assay approach.[37] This system will be further discussed in Chapter 2.

1.3.3 Zinc salophen in catalysis

A sophisticated example regarding the use of Zn(II)-salophen in catalysis is the resorcin[4]arene **4** fused to a salophen moiety reported by Rebek (Figure 6). This molecule was able to accelerate the hydrolysis of the *para*-nitrophenyl choline carbonate (PNPCC).[38] Energy minimized structure of the complex and the PNPCC suggested the occurrence of a simultaneous cation-π interaction and a C=O···Zn coordination bond. The supramolecular catalyst showed higher reactivity compared with the Zn(II)-salophen without the cavity. Also, the hydrolysis of a substrate lacking the ammonium "knob" is not catalyzed by **4**, highlighting the importance of the binding event into the cavity. This system will be further discussed in Chapter 3. The same molecule was demonstrated to be able to catalyze the synthesis of acetylcholine from choline and acetic anhydride (Figure 6, right).[39]

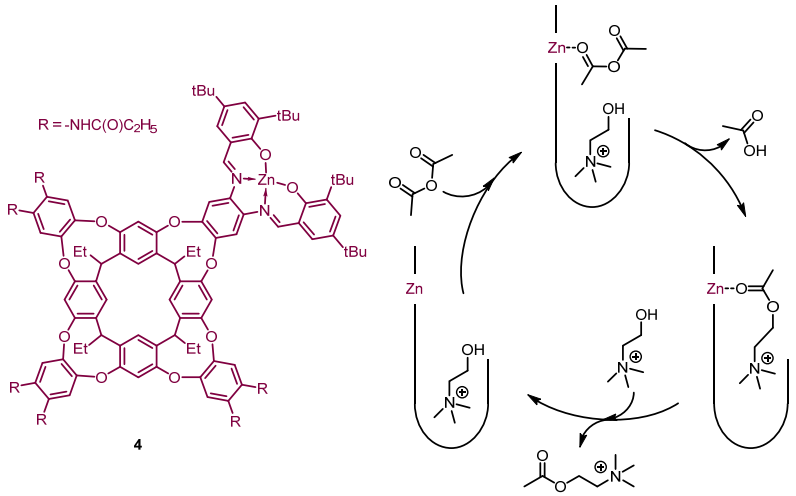

Figure 6. Resorcin[4]arene fused to a Zn(II)-salophen moiety reported by Rebek exploited for the hydrolysis of the PNPCC and synthesis of acetylcholine, left. Mechanism proposed for the synthesis of acetylcholine from choline and acetic anhydride, right.

Reek and co-workers exploited the Zn(II)-salophen functionality for the construction of encapsulated transition metal catalyst. Pyridylphosphanes and Zn(II)-salophen complexes could form higher order assemblies through N_{pyr}-Zn coordination. This supramolecular assembly could encapsulate rhodium and participate in the hydroformylation of 1-octene.[40]

One year later, the same group, reported the usage of a bis-Zn(II)-salophen as template in the formation of chelating heterobidentate ligands by self-assembly of two different monodentate ligands, **5** (Figure 7, left). These assemblies were studied in the rhodium-catalyzed asymmetric hydroformilation of styrene. Control experiments using homocombination of the ligands or combination of the ligands in the absence of the template gave lower values in term of conversion and/or enantioselectivity.[41,42] Recently the same group reported the construction of a supramolecular "box", **6**, constituted of a bis-Zn(II)-salophen derivative and a chiral phosphorus ligand functionalized with pyridine moieties (Figure 7, right).

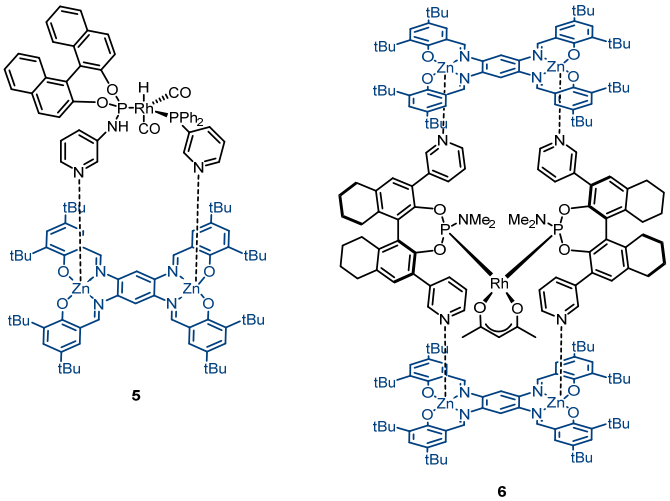

Figure 7. Supramolecular catalysts developed by Reek and co-workers involving the use of bis-Zn(II)-salophen as template. Left: template heterobidentate complex; Right: confined rhodium catalyst for the asymmetric hydroformylation of unfunctionalised internal alkenes.

This extremely robust 2+2 assembly was tested in the Rh-catalyzed asymmetric hydroformylation of cis- and trans-2-alkenes. In the presence of chiral ligand **6** the innermost aldehyde was produced preferentially with good enantioselectivity. The confinement in the active site was proposed by the authors as the main reason for the observed selectivity.[43]

Recently, Kleij and co-workers, used Zn(II)-salophen **7** as catalyst in the cycloaddition of carbon dioxide to terminal epoxides to obtain cyclic carbonates. The scope was quite broad and the reaction could be performed in mild conditions.[44] Later on, Kleij and Pescaramona could achieve higher catalytic efficiencies working in green CO_2 medium, *i.e.* solvent-free conditions.[45] The mechanism proposed by the authors involved coordination of the epoxide to the zinc metal center as the first step, followed by ring opening of the epoxide by the halide anion (co-catalyst). Then insertion of the CO_2 in the Zn-$O_{epoxyde}$ bond and carbonate cyclization (Figure 8).

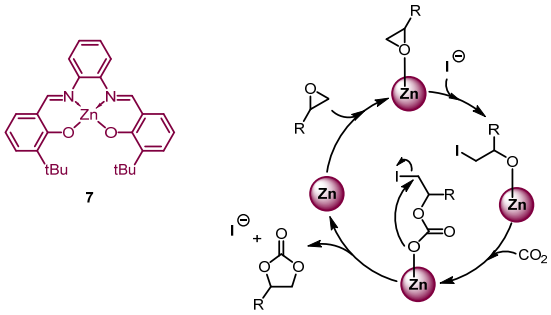

Figure 8. Zinc salophen complex used by Kleij in the synthesis of carbonates. Left: mechanism proposed for the Zn(II)-salophen catalyzed cycloaddition of CO_2 to oxiranes.

1.3.4 Zinc salophen in material chemistry

Thanks to the high Lewis acidity of the zinc metal center, Zn(II)-salophens provide useful synthons for the construction of supramolecular boxes.

In 2005 Reek reported the construction of supramolecular box assemblies, **8** and **9**, exploiting the strong N_{pyr} -Zn interaction. A series of supramolecular boxes based on bis-salophen and axial bipyridine ligands were reported (Figure 9). Luckily these structures easily crystallized, allowing a complete characterization through X-Ray analysis.[46] This porous material has the advantage that is formed by neutral building blocks and the channels were not blocked by counterions. The authors also reported that when smaller ditopic ligands were present, the formation of coordination polymers occurred preferentially.[47]

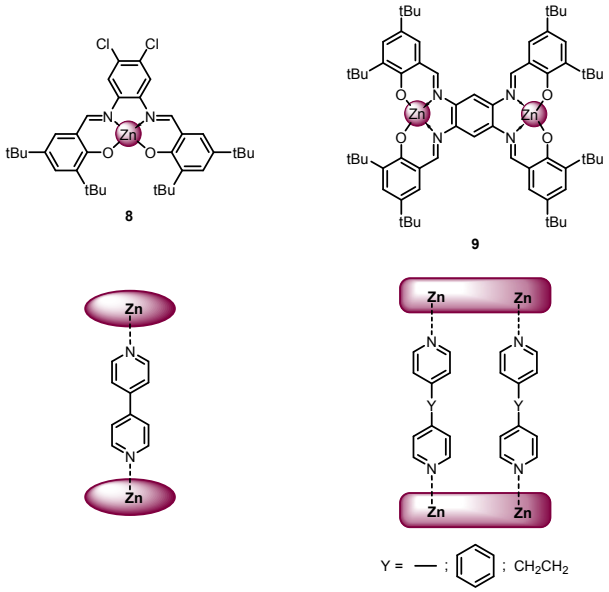

Figure 9. Supramolecular assemblies formed by mono- and bis-Zn(II)-salophen with ditopic amines.

Few years later, the same authors, described a Zn(II)-salpyr building block that self-assembled in a molecular vase structure. Again, the guiding force was the highly favorable N_{pyr} -Zn interaction. The tetrameric assembly was spontaneously formed in solution thanks to the presence of both Lewis acid (the zinc metal center) and Lewis base (the pyridine ring) in the salophen skeleton.[48]

Zinc and nickel salophen complexes were also tested in the field of metal-organic frameworks (MOFs). Mastalerz *et al.* could obtain a polymeric porous material, **10**, from the condensation of a tetrakis salicylaldehyde and *o*-phenylenediamine in the presence of the metal acetate salt. The resultant metal-functionalized porous organic framework showed selective gas adsorption properties (Scheme 2).[49]

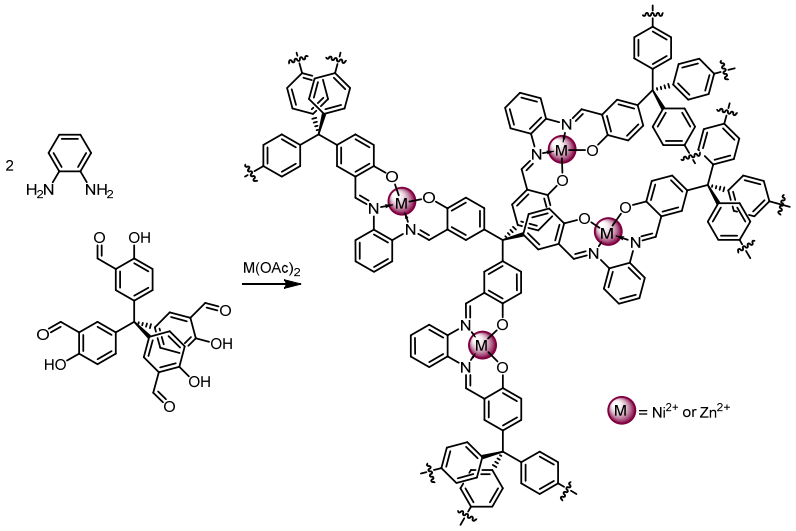

Scheme 2. Reaction of formation of the salophen covalent organic framework described by Mastalerz *et al.*

Because of the five-coordinate square pyramidal geometry of the zinc atom, Zn(II)-salophen complexes tend to dimerize in non-coordinating solvents (chloroform, dichloromethane, toluene, etc.) in the absence of a donor guest. The dimerization occurs through the axial coordination of the phenolic oxygen of one molecule with the zinc atom of an adjacent molecule and gives rise to a Zn-O-Zn-O square (Figure 10).[50]

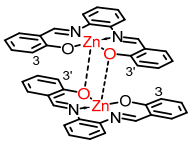

Figure 10. Line drawing structure showing the formation of the Zn(II)-salophen dimer mediated by Zn···O interactions.

Dimer formation was investigated both in solution and in the solid state varying the substitution on the salicylaldehyde rings. In particular, the substitution on the 3- and 3′-positions is crucial.[51] The aggregation/disaggregation properties of amphiphilic Zn(II)-salophen were

deeply investigated by Consiglio *et al*. The effect of the solvent was comprehensively studied and the absorption/emission spectra at different concentrations were recorded.[52]

The tendency of Zn(II)-salophen to dimerize was also exploited in the field of functional materials. In 2007 MacLachlan reported the formation of gels and nanofibers promoted by Zn···O interactions between adjacent salophen complexes. The gel formed in toluene and other aromatic solvents could be disrupted by the addition of pyridine that coordinated the zinc. The presence of bulky tert-butyl groups in the 3- and 3'-positions of the salophen skeleton prevented the formation of the gel.[53]

More recently, Di Bella and co-workers investigated a series of Zn(II)-salophen functionalized with alkoxy substituents able to self-assemble into nanofibers. The effect of the solvent in the formation of the nanofibers was evaluated and according to the authors the driving force for the formation of the supramolecular aggregates was dominated, again, by intermolecular Zn···O interactions (Figure 11).[54]

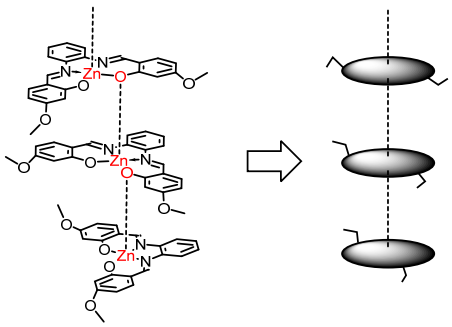

Figure 11. Schematic representation of the nanofibers studied by Di Bella.

1.4 Aim of this thesis

Thanks to the unique properties of Zn(II)-salophen complexes, many different application can be explored. Their versatility and synthetic accessibility allow an easy derivatization with specific functional groups to impart them the desired behavior.

We focused our attention on three fields: recognition of anions, catalysis and supramolecular gels.

In Chapter 2 is described our attempt to prepare a fluorescent receptor for anions based on a Zn(II)-salophen skeleton. To achieve this goal, we designed and prepared and non-symmetrically substituted Zn(II)-salophen covalently decorated with a 1,8-naphthalimide unit, a well know fluorophore. Unfortunately, from the comprehensive study we performed, it resulted that the attachment of the 1,8-naphthalimide unit to the Zn(II)-salophen complex provokes a significant emission quenching of the former one. To explain this phenomenon, we proposed and demonstrated the existence of a photoinduced energy transfer process between the naphthalimide unit (donor) and the salophen (acceptor).

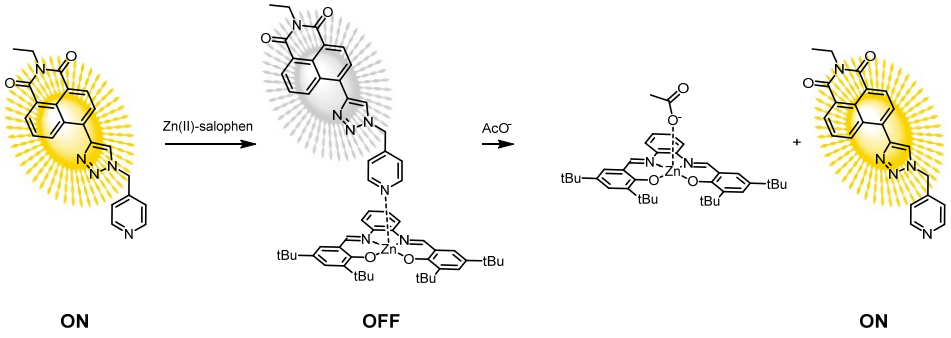

Figure 12. Schematic representation of the on-off-on fluorescent receptor for anions described in Chapter 2.

However, from our studies we cannot exclude the existence of a photoinduced electron transfer as an alternative pathway for emission deactivation.

On the basis of these findings, we developed a supramolecular system characterized by the presence of the two fluorophores and exploited the strong emission quenching experienced by the naphthalimide component to detect anions (*e.g.* acetate) by means of a typical "turn-on" fluorescent indicator displacement assay (Figure 12).

This study has been published in *Eur. J. Inorg. Chem.* **2015**, 2664-2670.

In Chapter 3 are reported our efforts in the development of a supramolecular catalyst bearing a binding site close to a catalytic group. We designed and synthesized an unprecedented resorcin[4]arene derivative featuring a Zn(II)-salophen unit covalently attached through a triazole ring (Figure 13). Resorcin[4]arenes cavitands are known to bind alkylammonium salts by cation-π interactions while Zn(II)-salophens can act as a Lewis acids activating a carbonyl group through an electrostatic C=O···Zn interaction. The synthesis was successfully completed and the final compound was characterized by means of mono- and bi-dimensional NMR, exact mass and X-ray analysis.

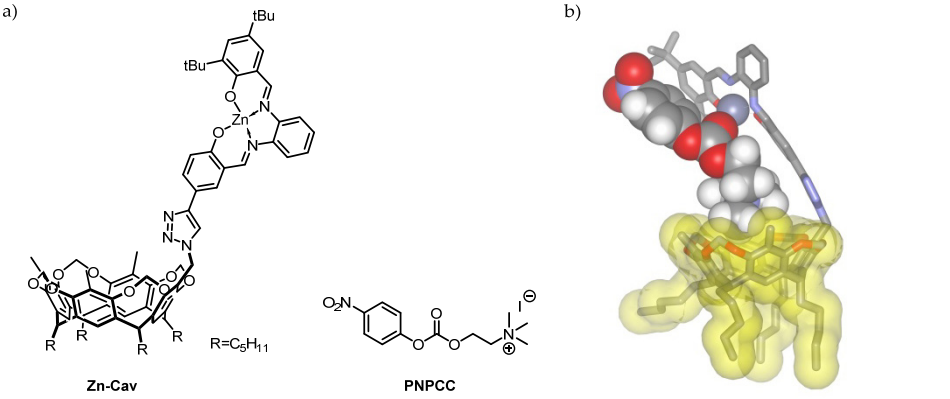

Figure 13. a) Line-drawing structure of the molecule synthetized **Zn-cav** (left) and *para*-nitrophenyl choline carbonate, PNPCC (right); b) energy-minimized complex **Zn-cav·PNPCC**.

On this derivative we performed kinetic studies of the hydrolysis of the *para*-nitrophenyl choline carbonate (PNPCC). The hydrolysis was followed by UV-vis spectroscopy, following the *para*-nitrophenolate absorbance. By comparison of the obtained results, a moderate increase in the reaction rate constant was detected in the presence of the catalyst. Model compounds were also tested in order to check the effectiveness of the catalytic performance of the molecule under study.

In Chapter 4 is described a project performed in collaboration with Prof. Beatriu Escuder (Universitat Jaume I, Castelló, Spain). We designed and prepared two peptides functionalized Zn(II)-salophens, **1a** and **1b** (Figure 14) and tested their gelation properties in different solvents.

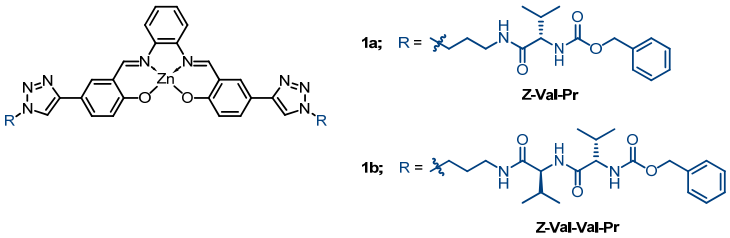

Figure 14. Line drawing structures of the molecules prepared and studied in Chapter 4.

Preliminary gelation experiments revealed the ability of **1b** to form a gel in acetonitrile when previously dissolved in small amounts of dimethyl sulfoxide (Figure 15).

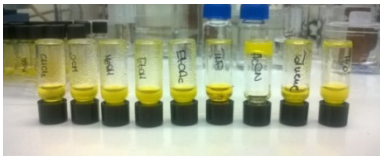

Figure 15. Picture of the tube inversion tests with gelator **1b** previously dissolved in DMSO.

Finally, the effect of the presence of a guest in the formation of the gel was evaluated. The obtained preliminary results gave an insight into the intermolecular interactions involved in the formation of the gel.

1.5 References

[1] J. M. Lehn, *Angew. Chem., Int. Ed. Engl.* **1988**, *27*, 89-112.
[2] J. M. Lehn, *Science* **1985**, *227*, 849-856.
[3] J. M. Lehn, *Pure Appl. Chem.* **1978**, *50*, 871-892.
[4] J. M. Lehn, *Angew. Chem., Int. Ed. Engl.* **1990**, *29*, 1304-1319.
[5] D. A. Leigh, V. Marcos, M. R. Wilson, *Acs Catalysis* **2014**, *4*, 4490-4497.
[6] M. D. Pluth, R. G. Bergman, K. N. Raymond, *Science* **2007**, *316*, 85-88.
[7] Min Hee Lee, J. S. K. and, J. L. Sessler, *Chem. Soc. Rev.* **2015**. DOI: 10.1039/C4CS00280F (Highlight).
[8] J. M. A. Carnall, C. A. Waudby, A. M. Belenguer, M. C. A. Stuart, J. J. P. Peyralans, S. Otto, *Science* **2010**, *327*, 1502-1506.
[9] A. Dalla Cort, P. De Bernardin, G. Forte, F. Y. Mihan, *Chem. Soc. Rev.* **2010**, *39*, 3863-3874.
[10] P. G. Cozzi, ibid.**2004**, *33*, 410-421.
[11] A. W. Kleij, *Chem. Eur. J.* **2008**, *14*, 10520-10529.
[12] W. Zhang, J. L. Loebach, S. R. Wilson, E. N. Jacobsen, *J. Am. Chem. Soc.* **1990**, *112*, 2801-2803.
[13] R. Irie, K. Noda, Y. Ito, N. Matsumoto, T. Katsuki, *Tetrahedron Lett.* **1990**, *31*, 7345-7348.
[14] L. E. Martinez, J. L. Leighton, D. H. Carsten, E. N. Jacobsen, *J. Am. Chem. Soc.* **1995**, *117*, 5897-5898.
[15] K. B. Hansen, J. L. Leighton, E. N. Jacobsen, ibid.**1996**, *118*, 10924-10925.
[16] E. N. Jacobsen, *Acc. Chem. Res.* **2000**, *33*, 421-431.
[17] R. G. Konsler, J. Karl, E. N. Jacobsen, *J. Am. Chem. Soc.* **1998**, *120*, 10780-10781.
[18] P. G. Cozzi, *Angew. Chem., Int. Ed. Engl.* **2003**, *42*, 2895-2898.
[19] J. Park, K. Lang, K. A. Abboud, S. Hong, *J. Am. Chem. Soc.* **2008**, *130*, 16484-16485.
[20] T. Kull, J. Cabrera, R. Peters, *Chem. Eur. J.* **2010**, *16*, 9132-9139.
[21] C. J. Whiteoak, G. Salassa, A. W. Kleij, *Chem. Soc. Rev.* **2012**, *41*, 622-631.
[22] V. V. Castelli, A. Dalla Cort, L. Mandolini, D. N. Reinhoudt, *J. Am. Chem. Soc.* **1998**, *120*, 12688-12689.
[23] V. V. Castelli, A. Dalla Cort, L. Mandolini, D. N. Reinhoudt, L. Schiaffino, *Eur. J. Org. Chem.* **2003**, 627-633.
[24] A. Dalla Cort, L. Mandolini, L. Schiaffino, *Chem. Commun.* **2005**, 3867-3869.
[25] V. Oliveri, A. Puglisi, G. Vecchio, *Dalton Trans.* **2011**, *40*, 2913-2919.
[26] V. Oliveri, G. Vecchio, *Eur. J. Med. Chem.* **2011**, *46*, 961-965.
[27] S. I. Vagin, R. Reichardt, S. Klaus, B. Rieger, *J. Am. Chem. Soc.* **2010**, *132*, 14367-14369.
[28] M. R. Broadley, P. J. White, J. P. Hammond, I. Zelko, A. Lux, *New Phytol.* **2007**, *173*, 677-702.
[29] A. Dalla Cort, L. Mandolini, C. Pasquini, K. Rissanen, L. Russo, L. Schiaffino, *New J. Chem.* **2007**, *31*, 1633-1638.
[30] E. C. Escudero-Adan, J. Benet-Buchholz, A. W. Kleij, *Inorg. Chem.* **2008**, *47*, 4256-4263.
[31] S. J. Wezenberg, E. C. Escudero-Adan, J. Benet-Buchholz, A. W. Kleij, *Org. Lett.* **2008**, *10*, 3311-3314.

[32] M. Cano, L. Rodriguez, J. C. Lima, F. Pina, A. D. Cort, C. Pasquini, L. Schiaffino, *Inorg. Chem.* **2009**, *48*, 6229-6235.
[33] A. D. Cort, P. De Bernardin, L. Schiaffino, *Chirality* **2009**, *21*, 104-109.
[34] S. J. Wezenberg, E. C. Escudero-Adan, J. Benet-Buchholz, A. W. Kleij, *Chem. Eur. J.* **2009**, *15*, 5695-5700.
[35] K. E. Splan, A. M. Massari, G. A. Morris, S. S. Sun, E. Reina, S. T. Nguyen, J. T. Hupp, *Eur. J. Inorg. Chem.* **2003**, 2348-2351.
[36] M. E. Germain, T. R. Vargo, P. G. Khalifah, M. J. Knapp, *Inorg. Chem.* **2007**, *46*, 4422-4429.
[37] M. Piccinno, G. Aragay, F. Y. Mihan, P. Ballester, A. Dalla Cort, *Eur. J. Inorg. Chem.* **2015**, 2664-2670.
[38] S. Richeter, J. Rebek, *J. Am. Chem. Soc.* **2004**, *126*, 16280-16281.
[39] F. H. Zelder, J. Rebek, *Chem. Commun.* **2006**, 753-754.
[40] A. W. Kleij, M. Lutz, A. L. Spek, P. W. N. M. van Leeuwen, J. N. H. Reek, ibid.**2005**, 3661-3663.
[41] M. Kuil, P. E. Goudriaan, P. W. N. M. van Leeuwen, J. N. H. Reek, ibid.**2006**, 4679-4681.
[42] M. Kuil, P. E. Goudriaan, A. W. Kleij, D. M. Tooke, A. L. Spek, P. W. N. M. van Leeuwen, J. N. H. Reek, *Dalton Trans.* **2007**, 2311-2320.
[43] T. Gadzikwa, R. Bellini, H. L. Dekker, J. N. H. Reek, *J. Am. Chem. Soc.* **2012**, *134*, 2860-2863.
[44] A. Decortes, M. M. Belmonte, J. Benet-Buchholz, A. W. Kleij, *Chem. Commun.* **2010**, *46*, 4580-4582.
[45] M. Taherimehr, A. Decortes, S. M. Al-Amsyar, W. Lueangchaichaweng, C. J. Whiteoak, E. C. Escudero-Adan, A. W. Kleij, P. P. Pescarmona, *Catal. Sci.Technol.* **2012**, *2*, 2231-2237.
[46] A. W. Kleij, M. Kuil, D. M. Tooke, M. Lutz, A. L. Spek, J. N. H. Reek, *Chem. Eur. J.* **2005**, *11*, 4743-4750.
[47] M. Kuil, I. M. Puijk, A. W. Kleij, D. M. Tooke, A. L. Spek, J. N. H. Reek, *Chem. Asian J.* **2009**, *4*, 50-57.
[48] A. W. Kleij, M. Kuil, D. M. Tooke, A. L. Spek, J. N. H. Reek, *Inorg. Chem.* **2007**, *46*, 5829-5831.
[49] M. Mastalerz, H. J. S. Hauswald, R. Stoll, *Chem. Commun.* **2012**, *48*, 130-132.
[50] A. W. Kleij, M. Kuil, M. Lutz, D. M. Tooke, A. L. Spek, P. C. J. Kamer, P. W. N. M. van Leeuwen, J. N. H. Reek, *Inorg. Chim. Acta* **2006**, *359*, 1807-1814.
[51] M. M. Belmonte, S. J. Wezenberg, R. M. Haak, D. Anselmo, E. C. Escudero-Adan, J. Benet-Buchholz, A. W. Kleij, *Dalton Trans.* **2010**, *39*, 4541-4550.
[52] G. Consiglio, S. Failla, P. Finocchiaro, I. P. Oliveri, R. Purrello, S. Di Bella, *Inorg. Chem.* **2010**, *49*, 5134-5142.
[53] J. K. H. Hui, Z. Yu, M. J. MacLachlan, *Angew. Chem., Int. Ed. Engl.* **2007**, *46*, 7980-7983.
[54] I. P. Oliveri, S. Failla, G. Malandrino, S. Di Bella, *J. Phys. Chem. C* **2013**, *117*, 15335-15341.

Chapter 2

Unexpected Emission Properties of a 1,8-Naphthalimide Unit Covalently Appended to a Zn-Salophen

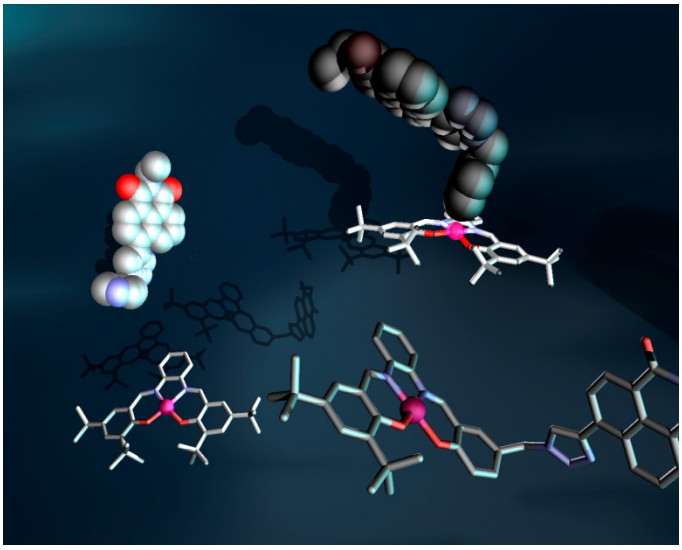

This study has been published in *Eur. J. Inorg. Chem.* **2015**, 2664-2670.

2.1 Introduction

The importance and ubiquity of anions in many chemical and biological processes have boosted the field of anion coordination chemistry research.[1,2,3] Anions are not only important in many sustaining life processes (*i.e.* enzymatic processes) but also represent a serious environmental problem (*e.g.* eutrophication).

Many elegant studies have been reported dealing with the development of optical sensors for anions and the understanding of their binding modes and sensing mechanisms.[1,4,5] Of particular interest are optical molecular probes based on a recognition site covalently linked to a chromophore/fluorophore unit.[6,7,8] In these systems, the recognition unit binds selectively the target species and the molecular recognition event is transduced through the modulation of the optical properties of the signaling unit (chromophore). For decades, chromogenic/absorbing organic dyes have been widely used as signaling units. Nowadays, however, fluorescent dyes are preferred because they provide increased sensitivity to the sensing methodology.[5,9]

In the last years, zinc-salophen complexes have attracted increasing attention owing to the Lewis acidity of the Zn(II) center that makes them excellent receptors for electron-rich substrates including neutral molecules and anions.[10] Such interesting properties come along with an easy synthetic access and reasonable chemical stability. The recognition event is generally monitored by absorption spectroscopy because the quantum yield of the Zn-salophen fluorescence is usually very low.[11,12] We envisaged that the decoration of the Zn-salophen scaffold with a highly fluorescent unit could produce a chemosensor able to signal the binding of target molecules to the Zn-center through changes in the emission properties of the attached chromophore. Our

goal was to increase the sensibility of the sensing system by changing the transduction of the binding event from absorption to fluorescence signaling. We focused our attention on the 1,8-naphthalimide fluorophore as reporter unit. The 1,8-naphthalimide unit is characterized by unique photophysical properties (*i.e.* high quantum yield), and straightforward tunability by simple modifications of the naphthalene skeleton and/or at the imide unit.[13] 1,8-naphthalimide based receptors covalently linked to Zn^{2+} complexes have already been reported in the literature.[14,15,16] Recognition of an anion or a cation by the binding center is able to modulate the emission properties of the naphthalimide fluorophore, giving rise to a signaling optical response.

Herein, we report the synthesis and characterization of a non-symmetrically substituted Zn-salophen complex having one 1,8-naphthalimide unit tethered by a triazole ring (**1a**, Figure 1).

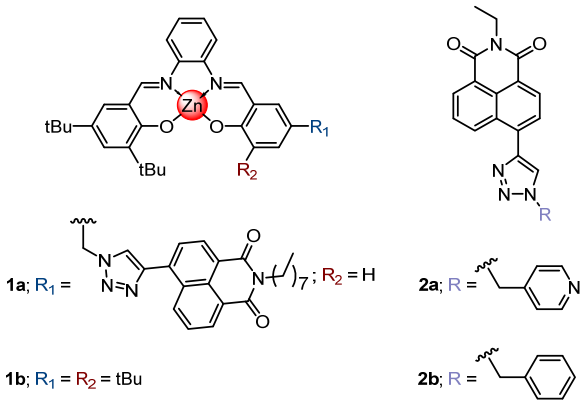

Figure 1. Line-drawing structures of the molecules prepared and studied in this work.

The presence of two tert-butyl groups in one half of the salophen unit of **1a** was aimed to prevent its dimerization through intermolecular Zn-O interactions.[17] On the other hand, the *N*-octyl chain introduced in the naphthalimide component served to increase the solubility of **1a** in organic solvents. We investigated the absorption and emission properties of **1a**, as well as its binding

properties towards acetate anion, used to test the behavior of the system in the presence of a coordinating anion. Our studies revealed unexpected features in the emission properties of **1a**, see paragraph 2.2.2 - *Emission spectroscopy studies of salophen **1a***. To rationalize such results, we designed and studied a supramolecular model system based on the pyridine naphthalimide derivative **2a** and the symmetrically substituted Zn-salophen **1b**. In solution, these components assembled into a 1:1 complex through axial coordination of the pyridine group of **2a** with the Zn metal center of **1b**. We describe the spectroscopic and thermodynamic characterization of the **1b•2a** complex. The obtained results with the supramolecular model **1b•2a** indicated that the quenching of the naphthalimide emission was caused by a photoinduced process that involved the Zn-salophen component. This result also explains the unexpected emission properties found for the naphthalimide unit in the covalently connected receptor **1a**.

2.2 Results and Discussion

2.2.1 Synthesis and characterization of Zn-salophen 1a

5-(azidomethyl)-2-hydroxybenzaldehyde **3** was obtained by reacting sodium azide with 5-(chloromethyl)-2-hydroxybenzaldehyde. On the other hand, commercially available 4-Bromo-1,8-naphthalic anhydride was first converted to the corresponding imide derivative. Then, an ethynyl substituent was introduced by Sonogashira coupling followed by deprotection of the trimethylsilyl group to finally afford the ethynyl-naphthalimide derivative **4** (See Experimental Section). Cu(I) catalyzed reaction of the azide salycilaldehyde derivative **3** with alkyne **4** afforded the 1,8-naphthalimide triazole **5** in 69% yield after column chromatography purification. The condensation reaction of

monoimine **6** with the functionalized salycilaldehyde **5** produced Zn-salophen **1a** as an orange solid in 75% yield (Scheme 1).

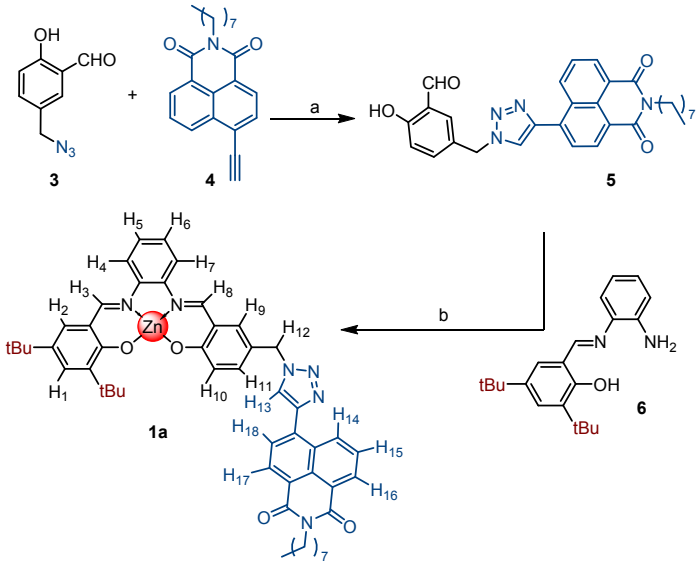

Scheme 1. Synthesis of non-symmetrical salophen **1a**. Reagents and conditions: a) $[Cu(CH_3CN)_4]PF_6$, TBTA, DMSO, room temperature, 48 h, 69%; b) $ZnCl_2$, Et_3N, DCM/MeOH 2:1, room temperature, 18 h, 75%.

The ^1H NMR spectrum of salophen **1a** in $CDCl_3$ solution displayed broad signals for the aromatic protons of the salophen core. Most likely, the broadening of the signals is caused by a chemical exchange process between monomer and dimer forms of **1a** that occurred at an intermediate rate on the chemical shift timescale. The tendency of Zn-salophen derivatives to dimerize at millimolar concentration in weak or non-coordinating solvents is well-known.[17]

Conversely, the ^1H NMR spectrum of **1a** in DMSO-d_6 solution showed sharp and well-defined proton signals, which were easily assigned using 2D NMR experiments. The imine protons H_3 and H_8 resonances appeared separately at δ = 8.99 and 8.94 ppm respectively, confirming the non-symmetrical nature of the Zn-salophen core. Moreover, the triazole proton H_{13} appeared as a sharp

singlet at δ = 8.89 ppm. NOE cross-peaks were observed between the triazole proton H_{13} and aromatic protons H_{14} and H_{18} present in the naphthalimide unit. This is an expected result if we consider the free rotation of the C-C bond connecting the triazole ring and the 1,8-naphthalimide unit.

A DOSY experiment performed on a DMSO-d_6 solution of **1a** at 298 K assigned a diffusion coefficient of 1.41×10^{-10} m^2/s to the molecule. This diffusion coefficient value corresponds to a hydrodynamic radii (r_{exp}) of 7.66 Å, which is in good agreement with the dimensions of the molecule estimated using molecular modeling (Figure 2).[18]

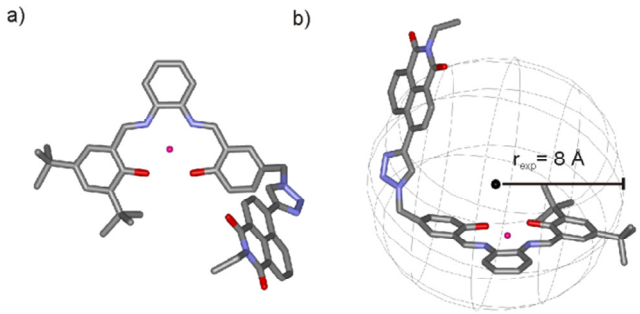

Figure 2. Top (a) and side (b) views of the MM3 energy minimized structure of salophen **1a** shown in stick representation. Non-polar hydrogen atoms are omitted for clarity. A sphere centered on **1a** and with a radii of 8 Å that corresponds to the value determined from the DOSY experiment is shown in (b).

2.2.2 Solution binding studies

Thermodynamic characterization of the complex of 1a with acetate anion.

Zinc-salophens are known to be good receptors for anions.[19,20] Preliminary studies to examine the behavior of **1a** in the presence of an anion were performed with acetate.

The interaction of **1a** with acetate was probed using ^1H NMR spectroscopy (Figure 3). The addition of incremental amounts of tetrabutylammonium acetate, TBA(AcO), to a ~1 mM solution of **1a** in $CDCl_3$ resulted in chemical

shift changes of its proton signals and the sharpening of some of them that initially were broad.

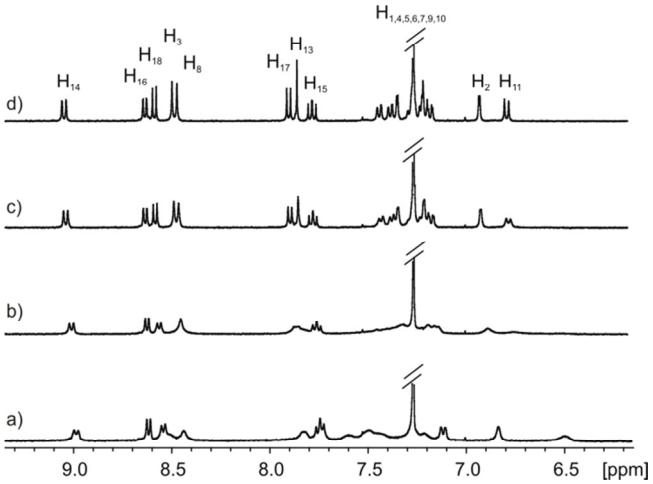

Figure 3. Selected region of the ^{1}H-NMR of **1a** in $CDCl_3$ (4.49×10^{-3} M) upon addition of 0 (a), 0.5 (b), 1 (c) and 1.5 (d) equivalents of TBA(AcO).

This observation confirmed that acetate anion coordinated to the zinc metal center of the salophen core of **1a** and disrupted its dimerization. The addition of more than 1 equivalent of acetate did not induce any additional change in the NMR spectra. We concluded that a 1:1 complex **1a•AcO**$^{-}$ is formed with an association constant higher than 10^4 M^{-1}. In order to assess an accurate stability constant value for the **1a•AcO**$^{-}$ complex we next performed a UV-Vis titration experiment.

The UV-Vis spectrum of the zinc-salophen **1a** in chloroform solution displayed two broad absorption bands with maxima centered at 300 nm and 365 nm, respectively. This spectrum closely resembles the sum of the absorption profiles of the two separated chromophores in **1b** and **2b**. Such result suggested that the electronic interaction of the two chromophores in the ground state of **1a** is weak (Figure 4).

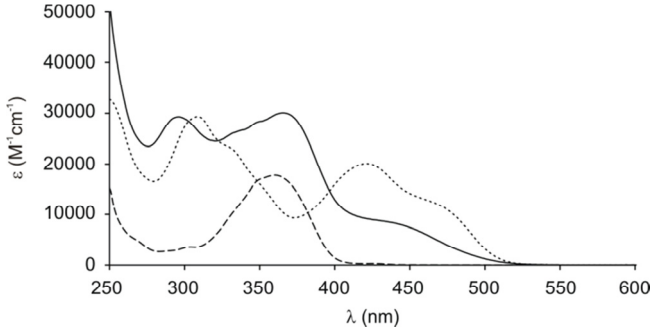

Figure 4. Absorption spectra in molar absorption coefficient scale of **1a** (solid line), **1b** (dotted line) and **2b** (dashed line) in chloroform.

A dilution experiment of **1a** in a range of concentrations of $10^{-7} \div 10^{-5}$ M showed that the absorption spectra in epsilon scale remained constant. Hence, in complete agreement with a previous report for a related system[21] we concluded that in this range of concentrations **1a** should exist in solution as a monomeric species.

The addition of increasing amounts of TBA(AcO) salt (0-6 eq) to a 10^{-5} M chloroform solution of **1a** caused the decrease of the absorption bands centered at 300 and 365 nm and the simultaneous appearance of a new band with a maximum at 405 nm (Figure 5).

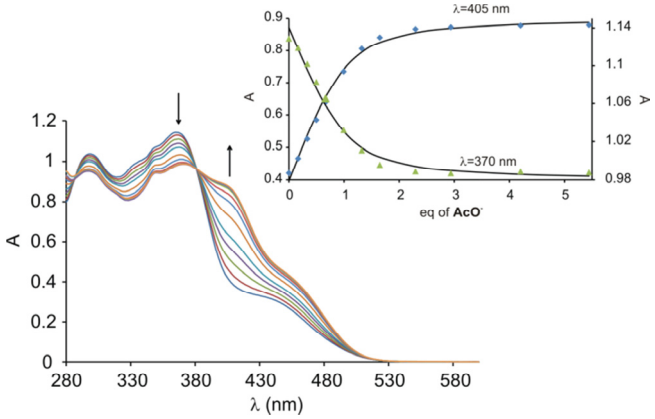

Figure 5. Absorption spectra of **1a** (3.69×10^{-5} M) upon addition of incremental amounts of AcO^- (0-6 eq) in chloroform. Inset: fit of the experimental data at 405 nm and 370 nm to the calculated theoretical binding curve for a 1:1 binding model considering two coloured species (free **1a** and **1a•AcO**$^-$ complex).

The titration spectra provided a clear isosbestic point centered at 380 nm suggesting the existence in solution of a single equilibrium involving the two species. Accordingly, the UV-Vis titration data were analyzed using a theoretical 1:1 binding model that considered two colored species (free **1a** and **1a•AcO**$^-$ complex). The fit was good and returned an association constant value of K_a = (1.73 ± 0.10)×10^5 M^{-1} for the **1a•AcO**$^-$ complex. The determined association constant value is in agreement with those reported for analogous zinc-salophen receptors binding acetate anion.[19]

Emission spectroscopy studies of salophen 1a.

The decoration of the salophen complex with the 1,8-naphthalimide unit was expected to improve the spectroscopic emission properties of the system and promote its use at low concentrations (10^{-6} – 10^{-7} M) to detect the presence of anions. To test this hypothesis we decided to study the complexation of acetate ion by **1a** at micromolar concentration using emission spectroscopy.

Figure 6 shows the emission spectrum in chloroform of **1a** (λ_{exc} = 360 nm). Two broad emission bands centered at 420 and 620 nm, respectively, are visible. By comparison with the emission spectra of **1b** and **2b** we attributed them to the separate emission of the two chromophores present in the structure of **1a**: the 1,8-naphthalimide (420 nm) and Zn-salophen (620 nm).

However, the 1,8-naphthalimide chromophore in **2b** is a significantly better emitter than zinc-salophen chromophore of **1b**, see Figure 6. In fact, the emission quantum yield (Φ_{em}) of the 1,8-naphthalimide chromophore **2b** was measured to be 0.8, much higher than the reported value for the zinc-salophen complex **1b**, Φ_{em} = 0.3.[22] Notably, the high emission exhibited by the 1,8-naphthalimide in **2b** is strongly quenched when the chromophore is covalently incorporated in the structure of **1a**. This indicates the existence of a

quenching mechanism for the naphthalimide unit emission in **1a**, *i.e.* photoinduced electron transfer (PET) or energy transfer (ET).

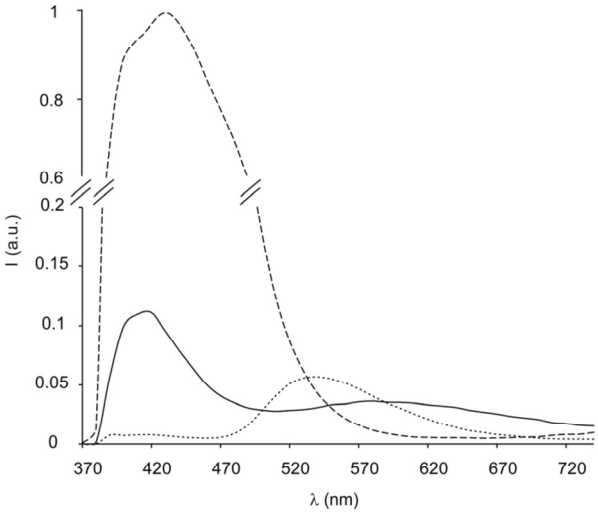

Figure 6. Emission spectra of **1a** (solid line, 1×10^{-6} M), **1b** (dotted line, 1×10^{-6} M) and **2b** (dashed line, 1×10^{-7} M) in chloroform λ_{ex} = 360 nm. Please notice the break in the scale of normalized emission intensity.

The emission spectrum of **1a** showed quite similar intensities for the bands assigned to the 1,8-naphthalimide and zinc-salophen units which did not match with the different quantum yield values observed for the two separated units. The observed unexpected quenching in the emission of the 1,8-naphthalimide covalently attached to the Zn-salophen in **1a** prompted us to further investigate the system by using a model in which the two chromophores were kept close in space through a coordinative bond, yielding a supramolecular complex.

2.2.3 Synthesis of the components of the supramolecular complex

Thermodynamic characterization of the complex.

The designed supramolecular system is based on the symmetrically substituted Zn-salophen **1b** and pyridine derivative **2a** decorated with a 1,8-naphthalimide unit (Figure 1). The Zn-salophen **1b** was synthesized following a procedure reported in literature.[23] Naphthalimides **2a** and **2b** were prepared by Cu(I)

catalyzed reactions of *N*-ethyl-6-ethynil-1,8-naphthalimide **S1** with 4-(azidomethyl)pyridine **S2** or benzyl azide **S3**, respectively (See Experimental Section).

Compounds **1b** and **2a** are expected to self-assemble in solution through axial coordination of the nitrogen atom of the pyridine-ligand to the Zn metal center. Based on literature precedents the association constant for the assembly **1b•2a** was estimated as ~ 10^5 M^{-1}.[24] Derivative **2b** was used as a control compound because clearly it cannot form a coordination complex with **1b**.

The ^{1}H NMR spectrum of **1b** in $CDCl_3$ showed broad proton signals (similar to **1a**) due to the dimerization process experienced by Zn-salophen at millimolar concentration in non-polar solvents (*vide supra*). When increasing amounts of **2a** were added to the solution of **1b**, the proton signals of the latter became sharper. No further changes were observed in the chemical shift values of **1b** when more than 1 equivalent of **2a** was added. These results indicated the disruption of the dimeric aggregates of **1b** and the formation a 1:1 coordination complex between **1b** and **2a** for which we assessed a binding constant higher than 10^4 M^{-1} in complete agreement with the previous estimate. In the early stages of the titration the proton signals corresponding to the pyridyl group of the naphthalimide **2a** appeared upfield shifted compared to those of free **2a**. Most likely, the magnetic anisotropy caused by the nearby Zn-salophen unit in the coordination complex **1b•2a** is responsible for the observed upfield shift.[24] A 2D-NOESY spectrum showed an intense cross peak between the protons α to the nitrogen atom of the pyridine ring in **2a** and those of the *tert*-butyl group in the salophen **1b** (Figure 7) thus providing support to the formation of the **1b•2a** supramolecular complex with axial coordination geometry.

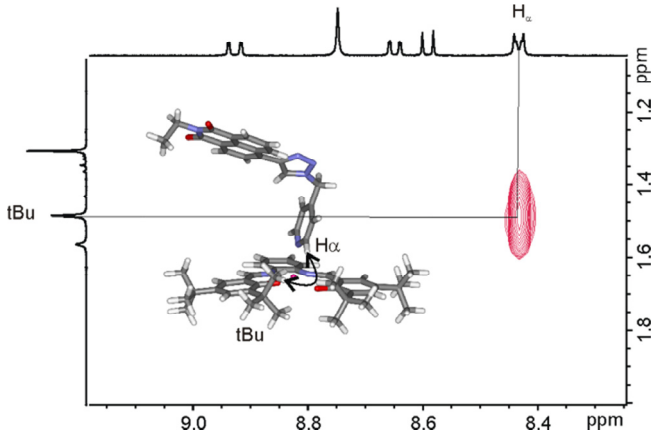

Figure 7. Selected area of the 2D NOESY spectrum of the 1:1 complex **1b•2a** in $CDCl_3$ solution . The MM3 energy minimized structure of the **1b•2a** complex is shown as an inset.

The interaction of **1b** with **2a** was also studied in chloroform using UV-Vis absorption spectroscopy. The coordination of the pyridine of **2a** to the Zn-salophen **1b** resulted in a slight increase and bathochromic shift of the absorption band at 420 nm ($\Delta\lambda$~6 nm), which is the expected behavior for the formation of an axial pyridine:Zn-salophen coordination complex.[23] The fit of the titration data to a 1:1 binding model was good and the calculated stability constant for the **1b•2a** complex was $K_a = (4.66 \pm 0.41) \times 10^5$ M^{-1}.

An analogous titration experiment performed with the reference compound **2b** did not produce noticeable changes in the absorption spectra of the Zn-salophen **1b**.

Emission properties of the supramolecular complex 1b•2a.

The emission spectra of the symmetrically substituted Zn-salophen **1b** (λ_{exc} = 360 nm) in chloroform solution displayed a weak band centered at 550 nm (Figure 6). In contrast, the separate emission spectra of compounds **2a** and **2b** showed strong bands with maxima at 420 and 430 nm, respectively.[25] The strong fluorescence shown by naphthalimides **2a** and **2b** indicated that

fluorescence quenching observed in **1a** was not caused by the intervention of the triazole ring connector.

The interaction of the pyridyl derivative **2a** with the symmetric Zn-salophen **1b** was probed also by emission spectroscopy. For practical reasons, we performed a reverse titration, where Zn-salophen **1b** was added to a 10^{-7} M chloroform solution of naphthalimide **2a**. We observed an intense quenching of the emission band of **2a** as the amount of **1b** in solution was increased. Conversely, the incremental addition of Zn-salophen **1b** to a solution of the reference naphthalimide **2b** had a negligible quenching effect on its emission. Taken together, these results indicated that the quenching of the emission of the 1,8-naphthalimide unit by the Zn-salophen required a spatio-temporal proximity of the two chromophores, naphthalimide and Zn-salophen. Using steady-state fluorescence experiments is not possible to unequivocally assign the nature of the quenching process that takes place in the **1b•2a** supramolecular complex. Interestingly, we observed that the emission spectrum of a solution containing **1b** and **2a** showed a slight increase in the emission band of the Zn-salophen (λ = 550 nm) compared to an analogous one containing **1b** and **2b** (Figure 8). In addition, the absorption band of the Zn-salophen **1b** centered at 420 nm perfectly overlaps the emission band of the 1,8-naphthalimide **2a**. All these observations suggested that the nature of the quenching process can be related to an energy transfer process. However, based on our results we cannot exclude the existence of a photoinduced electron transfer process as responsible of the quenching.[26]

The strong overlap that existed between the absorption spectra of the two chromophores did not allow the selective excitation of one of them. This limitation prevents the possibility to unequivocally demonstrate the energy transfer process.

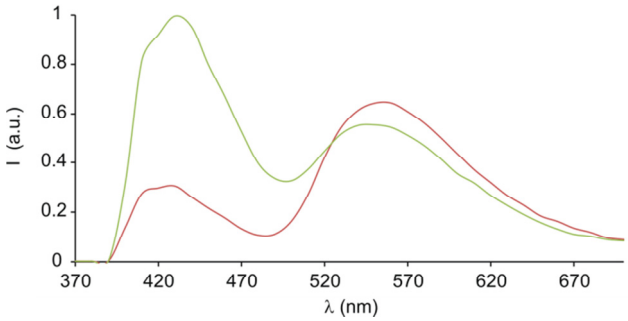

Figure 8. Comparison of the emission spectra at the final point of the titration of a solution of **2a** (red line, 6.62×10-7 M) and **2b** (green line, 6.84×10-7 M) with 11 eq of **1b**. λ_{ex} = 310 nm.[27]

In close analogy to the results obtained in the supramolecular **1b•2a** complex, we assigned the unexpected emission properties featured by the naphthalimide unit of the receptor **1a** in chloroform solution to the existence of a photoinduced quenching process (ET or PET) with the Zn-salophen moiety.

2.2.4 Sensing studies

Although the emission properties of receptor **1a** were not the expected ones, we decided to test its behavior in the presence of acetate using emission spectroscopy. Our expectation was that the binding of a coordinating anion to receptor **1a** could be transduced in changes in the emission properties of the naphthalimide unit (*e.g.* fluorescence restore). As shown in Figure 9a, the addition of 10 equivalents of TBA(AcO) to a micromolar solution of **1a** caused a hypsochromic shift of the emission band corresponding to the salophen unit. Unfortunately, the photoinduced process responsible for the quenching of the naphthalimide fluorescence in **1a** (*i.e.* electron or energy transfer) was not strongly influenced by acetate binding.

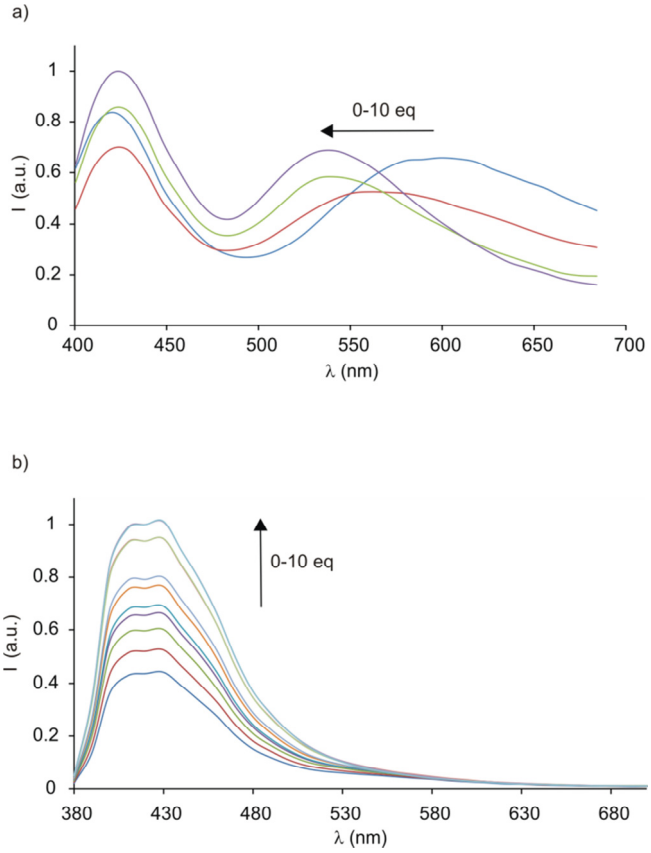

Figure 9. (a) Changes observed in the emission spectra of **1a** (1.51×10^{-6} M) in chloroform solution upon addition of acetate (0-10 eq). λ_{ex} = 380 nm. (b) Recovery of fluorescence emission upon addition of acetate anion (as tetrabutylammonium salt, 0-10 eq) to a chloroform solution of **2a** (8.29×10^{-6} M) and **1b** (1.75×10^{-5} M). λ_{ex} = 360 nm.

Finally, we studied the behavior of the supramolecular complex **1b•2a** as a "turn-on"-fluorescent sensor-ensemble for the detection of anions. In this case, the addition of the acetate anion (0 to 10 eq) to the solution containing the partially assembled **1b•2a** complex caused an increase in the emission of the 1,8-naphthalimide unit (Figure 9b). This observation is in complete agreement with the displacement of the pyridine-functionalized naphthalimide **2a** in the **1b•2a** complex by the acetate anion yielding the **1b•AcO**$^-$ complex. The reported association constant for Zn-salophen **1b•AcO**$^-$ complex is one order of

magnitude higher than the one we calculated for the **1b•2a** complex.[19] Therefore, acetate effectively competes with the pyridine-functionalized 1,8-naphthalimide bound to the Zn-salophen. The free naphthalimide **2b** that is released to the bulk solution recovers its emission properties.

2.3 Conclusions

In conclusion, we have synthesized a Zn-salophen receptor, **1a**, covalently decorated with a 1,8-naphthalimide unit. We have shown that the attachment of the Zn-salophen to a 1,8-naphthalimide provokes a significant quenching in the emission of the latter. We have also designed and characterized a supramolecular system based on the symmetric Zn-salophen **1b** and the 1,8-naphthalimide pyridyl derivative **2a**. In chloroform the two components form a 1:1 complex in which the pyridyl residue is axially coordinated to the Zn-salophen. By means of UV-Vis titrations, we determined the association constant of the **1b•2a** complex to be K_a = (4.66± 0.41)×10^5 M^{-1}. Interestingly, the emission of the naphthalimide **2a** is also quenched upon formation of the **1b•2a** complex. The results of the investigation of the emission properties of the supramolecular system **1b•2a** suggested that a photoinduced energy transfer process could be responsible for the quenching of the naphthalimide unit. We ascribed the existence of a similar photoinduced process in the covalently linked structure of receptor **1a** to explain the observed quenching of the fluorophore component. Unfortunately, the performed steady-state fluorescent experiments were not suitable to discard the existence of a photoinduced electron transfer between chromophores as an alternative pathway for emission deactivation.

The Zn-salophen receptor **1a** equipped with the naphthalimide unit transduces the binding of acetate anions to the Zn-center in significant changes of the

UV-Vis absorption spectrum. Conversely, the emission properties of **1a** are almost unaffected by the recognition event. Finally, we used the supramolecular system **1b•2a** as a "turn-on"-fluorescent sensor ensemble in which the presence of the anion was signaled through a typical indicator displacement assay.

2.4 Experimental Section

General Methods and Instrumentations

Reagents and solvents were obtained from commercial suppliers and used without further purification. Spectrophotometric grade chloroform containing amylene as stabilizer was purchased from Sigma Aldrich and freshly deacidified with basic aluminum oxide before each UV-Vis measurement. The ^{1}H and ^{13}C NMR spectra were recorded at 300MHz, 400 MHz or 500 MHz for ^{1}H or at 75 MHz, 100 MHz and 125 MHz for ^{13}C, respectively. The chemical shifts (δ) for ^{1}H and ^{13}C are given in ppm relative to residual signals of the solvents ($CHCl_3$, δ = 7.26 ppm for ^{1}H NMR, δ = 77.16 ppm for ^{13}C NMR or DMSO, δ = 2.50 ppm for ^{1}H NMR, δ = 39.52 ppm for ^{13}C NMR). When necessary, ^{1}H and ^{13}C signals were assigned by means of COSY, HSQC, NOESY and ROESY 2D-NMR sequences. High-resolution mass spectra (HRMS) were obtained on MicroTOF II from Bruker Daltonics (HPLC-MS-TOF) with positive ionization mode (ESI+). UV-Vis measurements were carried out on a Shimadzu UV-2401PC spectrophotometer equipped with a photomultiplier detector, double beam optics, and D2 and W light sources. Fluorescence measurements were performed in a Spectrofluorimeter Fluorolog Horiba Jobin Yvon. Dilute solutions ($A < 0.05$) were prepared in order to minimize inner filter effects.

Fluorescence quantum yield for naphthalimide **2a** was determined by using quinine sulphate in 0.1 N (0.05 M) sulphuric acid solution as reference standard ($\Phi = 0.53$).[28]

The determination of the unknown quantum yields was performed by comparing the absorption and the integrated fluorescence intensity of solutions whose absorbance is maintained below 0.05 at the excitation wavelength (350 nm). The unknown quantum yield was then calculated applying Eq 1.

$$\Phi_X = \Phi_{ST}\left(\frac{grad_X}{grad_{ST}}\right)\left(\frac{n^2_X}{n^2_{ST}}\right) \quad (1)$$

Where *X* and *ST* are the sample and the standard, respectively; Φ is the fluorescence quantum yield; *grad* is the gradient of the plot of the integrated fluorescence intensity *vs* absorbance; and *n* is the refractive index of the solvent (*X* = $CHCl_3$ *n* = 1.45, *ST* = H_2SO_4 0.1 N, *n* = 1.35).

Synthesis and characterization

Monoamine **6**[29], Zinc-salophen **1b**[30], 5-(chloromethyl)-2-hydroxybenzaldehyde[31], 5-(azidomethyl)-2-hydroxybenzaldehyde **3**[32], 2-ethyl-6-ethynyl-*1H*-benzo[*de*]isoquinoline-1,3(*2H*)-dione **S1**[33], 6-bromo-2-octyl-*1H*-benzo[*de*]isoquinoline-1,3(*2H*)-dione[34] and (azidomethyl)benzene **S3**[35], were prepared according to previously reported procedures.

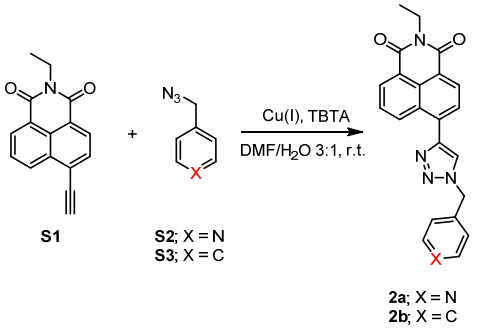

S1 **S2**; X = N **S3**; X = C **2a**; X = N **2b**; X = C

Synthesis of 2-octyl-6-(ethynyl)-*1H*-benzo[*de*]isoquinoline-1,3(2*H*)-dione (4). 6-bromo-2-octyl-*1H*-benzo[*de*]isoquinoline-1,3(*2H*)-dione (1g, 2.58 mmol), $Pd(PPh_3)_2Cl_2$ (0.36g, 0.052 mmol), CuI (0.02 g, 0.103 mmol) and PPh_3 (0.027 g, 0.103 mmol) were added in a round bottom flask and vacuum/argon cycles were performed. Then, dry Et_3N (4 mL) and dry THF (10 mL) were added. Finally ethynyltrimethylsilane (0.51 mL, 3.61 mmol) was added drop wise. The reaction was refluxed for 6 hours and after that time cooled down. The black oil was solubilized in $CHCl_3$ and washed with water. The crude was partially purified on a silica column (Hex/EtOAc 20:1). The trimethylsilyl compound (0.95 g, 2.35 mmol) was dissolved in MeOH (60 mL) at 60ºC and TBAF 1M in THF (8.4 mL, 8.4 mmol) was added. The reaction was stirred at 60ºC for 60 minutes and monitored by TLC. After 1 hour the reaction was cooled down, diluted with water and extracted with EtOAc. The organic layers were collected, dried on Na_2SO_4 and the solvent was removed under vacuum. The solid was purified on silica (Hex/CH_2Cl_2 10:1). Yield 79%. The ^1H NMR and ^{13}C-NMR are coincident with the one previously reported.[36]

Synthesis of 2-hydroxy-5-((4-(2-octyl-1,3-dioxo-2,3-dihydro-*1H*-benzo[*de*]isoquinolin-6-yl)-*1H*-1,2,3-triazol-1-yl)methyl)benzaldehyde (5). 6-ethynyl-2-octyl-1H-benzo[de]isoquinoline-1,3(2H)-dione **4** (0.5 g, 1.5 mmol) was solubilized in DMSO (10 mL) and 5-(azidomethyl)-2-hydroxybenzaldehyde (0.27 g, 1.5 mmol), $[Cu(CH_3CN)_4]PF_6$ (11 mg, 0.03 mmol), tris((1-benzyl-1H-1,2,3-triazol-4-yl)methyl)amine (8 mg, 0.015 mmol) were added. The reaction was left 48h at room temperature. Then the mixture was diluted in EtOAc (20mL) and washed with water. The crude was purified by silica column using CH_2Cl_2/Hex 10:1 to CH_2Cl_2/AcOEt 10:1 as eluent. Yield 69%.

^1H NMR (400 MHz, $CDCl_3$) δ 11.11 (s, 1H), 9.94 (s, 1H), 9.02 (dd, J = 8.6, 1.2 Hz, 1H), 8.65 (dd, J = 7.3, 1.2 Hz, 1H), 8.60 (d, J = 7.6 Hz, 1H), 7.92 (s, 1H), 7.90 (d, J =

7.6 Hz, 1H), 7.80 (dd, J = 8.6, 7.3 Hz, 1H), 7.66 (d, J = 2.4 Hz, 1H), 7.60 (dd, J = 8.6, 2.4 Hz, 1H), 7.09 (d, J = 8.6 Hz, 1H), 5.68 (s, 2H), 4.23 - 4.14 (m, 2H), 1.81 - 1.68 (m, 2H), 1.48 - 1.21 (m, 10H), 0.92 - 0.83 (m, 3H).

Synthesis of Zn-Salophen 1a. Aldehyde **5** (113 mg, 0.221 mmol) was solubilized in 3 mL of CH_2Cl_2 and a solution of the Monoimine **6** (71.8 mg, 0.221 mmol) in CH_2Cl_2 (2 mL) was added. $ZnCl_2$ (33.2 mg, 0.243 mmol) was solubilized in 2.5 mL of MeOH and added to the reaction mixture. Finally 30 μL of Et_3N were added. The reaction was stirred for 18h at room temperature. The solvent was partially evaporated and the flask was stored at -20º. After 1 hour the solid was filtered and washed with cold MeOH. The pure compound was obtained as an orange solid in a 75% of yield.

^{1}H NMR (500 MHz, DMSO-d_6) δ 9.17 (d, *J* = 8.6 Hz, 1H), 8.99 (s, 1H), 8.94 (s, 1H), 8.89 (s, 1H), 8.55 (d, *J* = 7.4 Hz, 1H), 8.53 (d, *J* = 7.8 Hz, 1H), 8.14 (d, *J* = 7.8 Hz, 1H), 7.93 (dd, *J* = 8.6, 7.4 Hz, 1H), 7.89 – 7.83 (m, 2H), 7.57 (d, *J* = 2.6 Hz, 1H), 7.42 – 7.32 (m, 3H), 7.31 (d, *J* = 2.8 Hz, 1H), 7.21 (d, *J* = 2.8 Hz, 1H), 6.70 (d, *J* = 8.8 Hz, 1H), 5.60 (s, 2H), 4.04 (m, 2H), 1.63 (m, 2H), 1.47 (s, 9H), 1.23-1.33 (m, 19H), 0.87 – 0.80 (m, 3H).

^{13}C NMR (125 MHz, DMSO) δ 172.46, 170.78, 164.06, 163.90, 163.58, 162.59, 145.31, 141.10, 140.56, 139.49, 136.79, 134.91, 134.49, 133.85, 133.06, 131.37, 130.95, 130.06, 128.98, 128.73, 128.65, 128.11, 127.97, 127.62, 127.11, 125.51, 124.39, 122.86, 122.02, 119.93, 119.51, 118.58, 116.95, 116.85, 53.60, 40.45, 40.36, 40.28, 40.20, 40.12, 40.03, 31.76, 30.04.

HRMS-MALDI+ *calc* for [M^+] 878.3492, found: 878.3493

Synthesis of 4-(azidomethyl)pyridine (S2). 4-(bromomethyl)pyridine hydrobromide (0.1 g, 0.395 mmol) was dissolved in 1 mL of DMF and potassium carbonate (55 mg, 0.395 mmol) was added and stirred 15 min. Then sodium azide (39 mg, 0.593 mmol) was added and the reaction was stirred for

3h at room temperature. CH_2Cl_2 and water were added to the mixture and the organic layer was separated. The aqueous layer was extracted with CH_2Cl_2 and the combined organic layers were washed with water. The organic layer was then dried over Na_2SO_4 and the solvent was evaporated. Quantitative yield.

^{1}H NMR (300 MHz, $CDCl_3$) δ 8.67 – 8.59 (m, 2H), 7.29 – 7.20 (m, 2H), 4.41 (s, 2H).

^{13}C NMR (100 MHz, $CDCl_3$) δ 150.30, 144.34, 122.34, 53.30.

HRMS-ESI+ *calcd* for [M+H$^+$]: 135.0665 found 135.0669.

Synthesis of 6-(1-benzyl-*1H*-1,2,3-triazol-4-yl)-2-ethyl-1H-benzo[*de*]isoquinoline-1,3(2*H*)-dione (2b). 2-ethyl-6-ethynyl-*1H*-benzo[*de*]isoquinoline-1,3(*2H*)-dione **S1** (32 mg, 0.128 mmol) was solubilized in 1.3 mL of DMF/water 3:1 and (azidomethyl)benzene **S3** (100 mg, 0.751 mmol), tris((1-benzyl-1H-1,2,3-triazol-4-yl)methyl)amine (0.7 mg, 1.284 μmol), $[Cu(CH_3CN)_4]PF_6$ (1 mg, 2.57 μmol) were added. The reaction was stirred 18h at room temperature. The reaction mixture then was poured into ice water and the yellow solid was filtrated, washed and dried. The product was obtained with a 79% yield.

^{1}H NMR (400 MHz, $CDCl_3$) δ 9.03 (dd, *J* = 8.6, 1.2 Hz, 1H), 8.65 (dd, *J* = 7.3, 1.2 Hz, 1H), 8.60 (d, *J* = 7.6 Hz, 1H), 7.89 (d, *J* = 7.6 Hz, 1H), 7.87 (s, 1H), 7.79 (dd, *J* = 8.6, 7.3 Hz, 1H), 7.50 – 7.30 (m, 5H), 5.69 (s, 2H), 4.26 (q, *J* = 7.1 Hz, 2H), 1.35 (t, *J* = 7.1 Hz, 3H).

^{13}C NMR (100 MHz, $CDCl_3$) δ 164.18, 163.90, 146.57, 134.34, 134.26, 132.88, 131.53, 130.74, 129.51, 129.42, 129.28, 128.99, 128.44, 127.53, 127.41, 123.32, 123.05, 122.75, 54.71, 35.71, 13.50.

HRMS-ESI+ *calcd* for [M+Na$^+$] 405.1322, found 405.1310.

Synthesis of 2-ethyl-6-(1-(pyridin-4-ylmethyl)-*1H*-1,2,3-triazol-4-yl)-1H-benzo[*de*]isoquinoline-1,3(2*H*)-dione (2a). 2-ethyl-6-ethynyl-1H-

benzo[de]isoquinoline-1,3(2H)-dione **S1** (28 mg, 0.112 mmol) was solubilized in 1.2 mL of DMF/water 3:1 and 4-(azidomethyl)pyridine **S2** (30 mg, 0.224 mmol), tris((1-benzyl-1H-1,2,3-triazol-4-yl)methyl)amine (0.6 mg, 1.123 μmol) and $[Cu(CH_3CN)_4]PF_6$ (0.8 mg, 2.247 μmol) were added. The reaction was stirred 18h at room temperature. Then the mixture was diluted with water and extracted with DCM. The aqueous layers were extracted with CH_2Cl_2 and the combined organic layers were washed with a solution of NH_4Cl and dried over Na_2SO_4. The compound was purified on silica column (eluent: CH_2Cl_2 /MeOH 1%). Yield 58%.

^{1}H NMR (400 MHz, $CDCl_3$) δ 9.00 (dd, *J* = 8.6, 1.2 Hz, 1H), 8.72 – 8.63 (m, 2H), 8.65 (dd, *J* = 7.3, 1.2 Hz, 1H), 8.61 (d, *J* = 7.6 Hz, 1H), 7.97 (s, 1H), 7.92 (d, *J* = 7.6 Hz, 1H), 7.80 (dd, *J* = 8.6, 7.3 Hz, 1H), 7.28 – 7.21 (m, 2H), 5.72 (s, 2H), 4.26 (q, *J* = 7.1 Hz, 2H), 1.35 (t, *J* = 7.1 Hz, 3H).

^{13}C NMR (100 MHz, $CDCl_3$) δ 164.09, 163.81, 150.96, 146.96, 143.22, 133.76, 132.60, 131.58, 130.70, 129.38, 128.99, 127.65, 127.52, 123.64, 123.13, 123.00, 122.41, 53.24, 35.74, 13.49.

HRMS-ESI+ *calcd* for $[M+H^+]$ 384.1455, found 384.1447.

2.5 References

[1] P. A. Gale, N. Busschaert, C. J. E. Haynes, L. E. Karagiannidis, I. L. Kirby, *Chem. Soc. Rev.* **2014**, *43*, 205-241.
[2] M. Boiocchi, M. Licchelli, M. Milani, A. Poggi, D. Sacchi, *Inorg. Chem.* **2015**, *54*, 47-58.
[3] A. Schaly, R. Belda, E. Garcia-Espana, S. Kubik, *Org. Lett.* **2013**, *15*, 6238-6241.
[4] P. A. Gale, C. Caltagirone, *Chem. Soc. Rev.* **2015**, *44*, 4212-4227.
[5] X. D. Lou, D. X. Ou, Q. Q. Li, Z. Li, *Chem. Commun.* **2012**, *48*, 8462-8477.
[6] A. P. de Silva, B. McCaughan, B. O. F. McKinney, M. Querol, *Dalton Trans.* **2003**, 1902-1913.
[7] M. H. Lee, J. S. Kim, J. L. Sessler, *Chem. Soc. Rev.* **2015**, *44*, 4185-4191.
[8] Y. Zhou, Z. Xu, J. Yoon, *Chem. Soc. Rev.* **2011**, *40*, 2222-2235.
[9] M. E. Moragues, R. Martinez-Manez, F. Sancenon, *Chem. Soc. Rev.* **2011**, *40*, 2593-2643.
[10] A. Dalla Cort, P. De Bernardin, G. Forte, F. Y. Mihan, *Chem. Soc. Rev.* **2010**, *39*, 3863-3874.
[11] K. L. Kuo, C. C. Huang, Y. C. Lin, *Dalton Trans.* **2008**, 3889-3898.
[12] K. H. Chang, C. C. Huang, Y. H. Liu, Y. H. Hu, P. T. Chou, Y. C. Lin, *Dalton Trans.* **2004**, 1731-1738.
[13] R. M. Duke, E. B. Veale, F. M. Pfeffer, P. E. Kruger, T. Gunnlaugsson, *Chem. Soc. Rev.* **2010**, *39*, 3936-3953.
[14] Z. C. Xu, K. H. Baek, H. N. Kim, J. N. Cui, X. H. Qian, D. R. Spring, I. Shin, J. Yoon, *J. Am. Chem. Soc.* **2010**, *132*, 601-610.
[15] A. J. Moro, P. J. Cywinski, S. Korsten, G. J. Mohr, *Chem. Commun.* **2010**, *46*, 1085-1087.
[16] J. F. Zhang, S. Kim, J. H. Han, S. J. Lee, T. Pradhan, Q. Y. Cao, S. J. Lee, C. Kang, J. S. Kim, *Org. Lett.* **2011**, *13*, 5294-5297.
[17] A. W. Kleij, M. Kuil, M. Lutz, D. M. Tooke, A. L. Spek, P. C. J. Kamer, P. W. N. M. van Leeuwen, J. N. H. Reek, *Inorg. Chim. Acta* **2006**, *359*, 1807-1814.
[18] The hydrodynamic radius (r_{exp}) was calculated from the experimental diffusion coefficient (D) using the Stokes Einstein relation (1).

$$r_{sph} = k_B T / 6\pi\eta D \quad (1)$$

Where k_B is the Boltzmann constant, T is the absolute temperature and η is the viscosity of the medium.
[19] S. J. Wezenberg, E. C. Escudero-Adan, J. Benet-Buchholz, A. W. Kleij, *Chem. Eur. J.* **2009**, *15*, 5695-5700.
[20] A. D. Cort, P. De Bernardin, L. Schiaffino, *Chirality* **2009**, *21*, 104-109.
[21] G. Consiglio, S. Failla, P. Finocchiaro, I. P. Oliveri, R. Purrello, S. Di Bella, *Inorg. Chem.* **2010**, *49*, 5134-5142.
[22] M. E. Germain, T. R. Vargo, P. G. Khalifah, M. J. Knapp, *Inorg. Chem.* **2007**, *46*, 4422-4429.
[23] A. Dalla Cort, L. Mandolini, C. Pasquini, K. Rissanen, L. Russo, L. Schiaffino, *New J. Chem.* **2007**, *31*, 1633-1638.
[24] E. C. Escudero-Adan, J. Benet-Buchholz, A. W. Kleij, *Eur. J. Inorg. Chem.* **2009**, 3562-3568.

[25] In order to compare the emission intensity of all the molecules under study (**1a**, **1b** and **2a** or **2b**), we selected an excitation wavelength at which all the molecules are excited.
[26] The relative energy levels of the frontier HOMO and LUMO orbitals of **1b** and **2a** were calculated at the B3LYP/6-31G theory level using a chloroform continuum solvent model PCM. The computed energy values were HOMO(**1b**): -5.32 eV, LUMO(**1b**): -2.03 eV, HOMO(**2a**): -6.39 eV and LUMO(**2a**): -2.70 eV. These energy values suggested that a photoinduced electron transfer process occurring from the HOMO of **1b** to the SOMO-1 of **2a** is thermodynamically viable. However, the results of these calculations were not sufficient to rule out the existence of an energy transfer process as an alternative mechanism of the emission quenching of **2a** in the **1b•2a** complex.
[27] The excitation wavelength was fixed at 310 nm in order to have a minimum direct excitation of the 1,8-naphthalimide units (**2a** or **2b**). This allowed to observe the emission band of the Zn-salophen **1b**, otherwise covered by the strong emission of the 1,8-naphthalimides.
[28] M. J. Adams, J. G. Highfield, G. F. Kirkbright, *Anal. Chem.* **1977**, *49*, 1850-1852.
[29] M. A. Munoz-Hernandez, T. S. Keizer, S. Parkin, B. Patrick, D. A. Atwood, *Organometallics* **2000**, *19*, 4416-4421.
[30] A. Dalla Cort, L. Mandolini, C. Pasquini, K. Rissanen, L. Russo, L. Schiaffino, *New J. Chem.* **2007**, *31*, 1633-1638.
[31] A. Dalla Cort, L. Mandolini, C. Pasquini, L. Schiaffino, *Org. Biomol. Chem.* **2006**, *4*, 4543-4546.
[32] V. Ayala, A. Corma, M. Iglesias, J. A. Rincon, F. Sanchez, *J. Catal.* **2004**, *224*, 170-177.
[33] M. Sawa, T. L. Hsu, T. Itoh, M. Sugiyama, S. R. Hanson, P. K. Vogt, C. H. Wong, *Proc. Natl. Acad. Sci. U. S. A.* **2006**, *103*, 12371-12376.
[34] Z. Chen, X. Liang, H. Y. Zhang, H. Xie, J. W. Liu, Y. F. Xu, W. P. Zhu, Y. Wang, X. Wang, S. Y. Tan, D. Kuang, X. H. Qian, *J. Med. Chem.* **2010**, *53*, 2589-2600.
[35] L. S. Campbell-Verduyn, L. Mirfeizi, R. A. Dierckx, P. H. Elsinga, B. L. Feringa, *Chem. Commun.* **2009**, 2139-2141.
[36] S. Lee, K. R. J. Thomas, S. Thayumanavan, C. J. Bardeen, *J. Phys. Chem. A* **2005**, *109*, 9767-9774.

Chapter 3

Hydrolysis of Carbonates Catalyzed by a Resorcin[4]arene Cavitand Decorated at the Upper rim with a Zn(II)-salophen

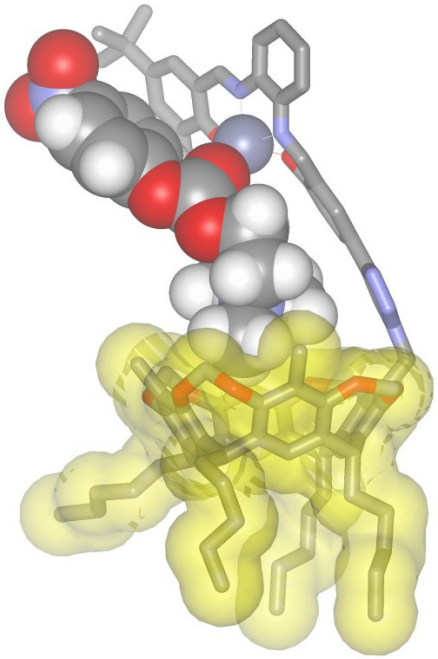

3.1 Introduction

Supramolecular catalysis is a discipline that aims to develop artificial enzymes, able to mimic the functions and the structures of natural enzymes (Figure 1).[1,2,3]

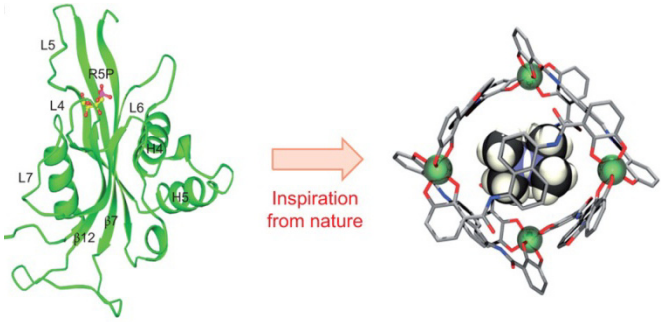

Figure 1. Representative example to show the concept of supramolecular catalysis.[4]

The growing interest in this field can be attributed to the important role of enzymes, sophisticated structures able to catalyze a number of reactions with high efficiency and substrate specificity.[5]

A key aspect in enzyme catalysis is the recognition of the substrate mediated by non-covalent interactions (*i.e.* hydrogen bonding, electrostatic, Lewis acid-Lewis base and hydrophobic ones). The progresses in both supramolecular chemistry and catalysis together with the proficiency in the modulation of non-covalent interactions are exploited in supramolecular catalysis were destabilization of the substrate ground state/stabilization of the transition state are the typical strategies adopted to increase the reaction rate.[1,6,7,8] Natural enzymes bind the appropriate substrate in the active site, generally in close proximity to the catalytic groups that decorate the binding pocket. Taking inspiration from this concept, sophisticated systems have been designed and prepared.[9,10]

Resorcin[4]arenes are generally obtained by acid-catalyzed condensation reaction of resorcinol with aldehydes (Scheme 1).[11,12] The resultant macrocycles

are quite conformationally flexible and the elaboration of their aromatic cavity by installing four methylene bridges at the upper rim reduces their conformational flexibility and produces *cavitands*, compounds with a permanent aromatic cavity.[13]

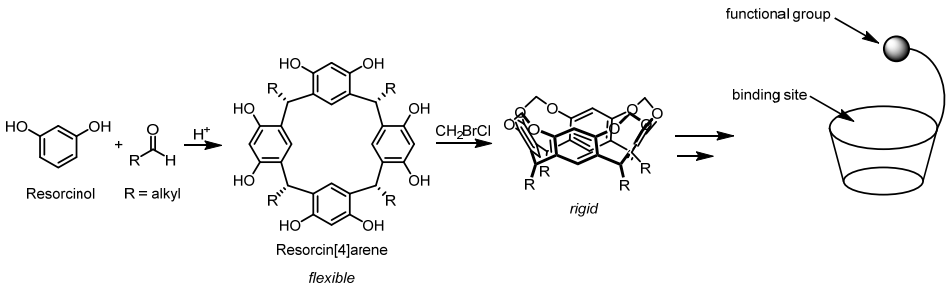

Scheme 1. Synthesis of a resorcinarene macrocycle and installation of the methylene bridges. Right: decoration of the cavity with a functional group.

Deep cavitands with extended aromatic walls, are able to bind small guests both in water and in organic solvents isolating them from the bulk solution.[14,15] Further decoration of these cavitands with appropriate functional groups provides molecules capable of performing specific functions, spreading from recognition to catalysis of diverse reactions.[9,16] In particular, the covalent linkage of a catalytic group close to the cavity affords enzyme-mimic structures which show catalytic activity in the hydrolysis/solvolysis of choline carbonates.[17,18,19,20,21]

In these systems the binding event is governed by cation-π interactions between the trimethylammonium group and the electron rich aromatic cavity of the macrocycle.[22,23]

Specifically, the functionalized resorcin[4]arene cavitand **4** (Chapter 1, Figure 6) fused to a Zn(II)-salophen complex was exploited by Rebek *et al.* as a catalyst both for the hydrolysis of the *para*-nitrophenyl choline carbonate (PNPCC) and for the synthesis of acetylcholine.[18,20] Zinc salophen complexes are in fact Lewis acids and are able to activate carbonyl groups through metal-ligand

interactions. In self-folding cavitands like **4** the ammonium group of choline is included deep inside of the aromatic cavity and the in-out exchange of the bound guest is kinetically slow on the chemical shift timescale. Moreover, the thermodynamic stability of the inclusion complex formed by the cavitand and the reaction product is highly stable thermodynamically resulting in not desirable catalyst inhibition.

Herein we report a novel resorcin[4]arene cavitand derivative, **Zn-cav**, featuring a Zn(II)-salophen unit attached covalently through a triazole ring at its upper rim (Figure 2). The resorcin[4]arene cavity is shallower than the ones previously reported, and this might be beneficious to speed up the kinetics of the host-guest equilibrium and increase the turn over frequency. In the design we also tried to gain some conformational flexibility by linking the catalytic group (*i.e.* the Zn(II)-salophen) through the insertion of a methylene unit. Conformational flexibility is in fact a fundamental aspect in enzymatic catalysis.[24] We report the synthesis of the cavitand derivative **Zn-cav** and disclose preliminary catalytic studies regarding its use as catalysts for the hydrolysis of carbonates.

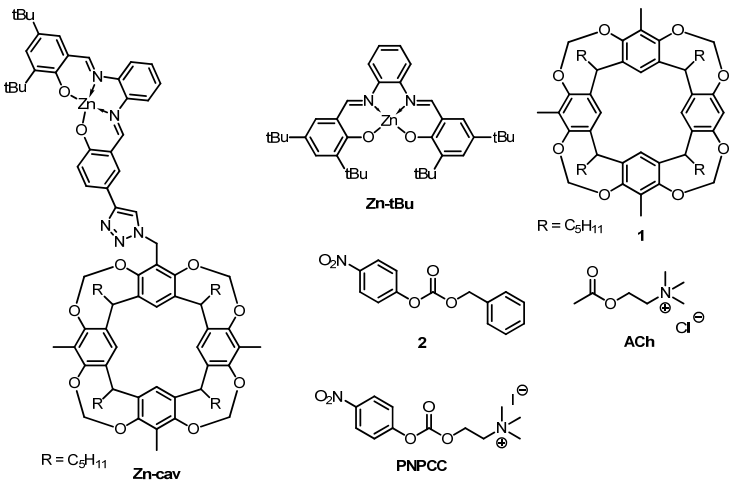

Figure 2. Line drawing structure of the molecules used in this study.

3.2 Results and Discussion

3.2.1 Synthesis and characterization of Zn-cav

Monobromo bridged resorcin[4]arene **3** (Scheme 2) was prepared in three steps following a previously reported procedure for similar compounds.[25,26] First, acid catalyzed condensation of methyl-resorcinol and hexanal gave resorcin[4]arene macrocicle. Then, reaction of the conformationally flexible macrocicle with CH_2BrCl allowed the installation of four methylene bridges between the phenolic oxygens of the resorcin[4]arene to afford cavitand **1** in high yield. Monobrominated methyl-resorcin[4]arene **3** was then prepared by reacting the bridged resorcinarene **1** with 1 equivalent of NBS. Despite the formation of a mixture of different brominated compounds (*i.e.* mono-, di-, tri-brominated), the desired mono-brominated derivative could be easily isolated by column chromatography. The bromine was subsequently substituted for an azide group upon reaction with NaN_3 affording the azido-derivative **4**.

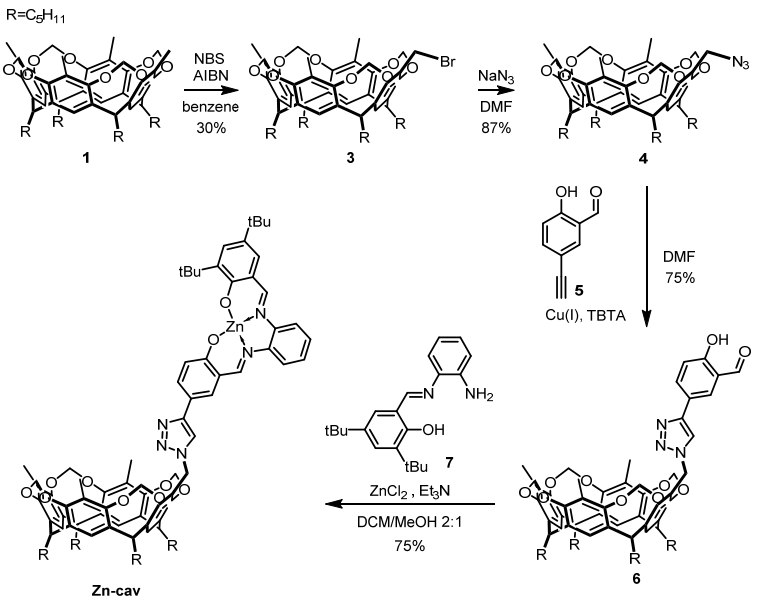

Scheme 2. Synthesis of Zn(II)-salophen functionalized resorcin[4]arene **Zn-cav**.

Finally, cavitand **4** underwent a copper-catalyzed azide–alkyne cycloaddition (CuAAC, click reaction) with 5-ethynyl-2-hydroxybenzaldehyde **5** to yield the hydroxyl aldehyde derivative **6**. Resorcin[4]arene cavitand **6** was reacted with the monoimine of the 3,5-di-*tert*-butyl-salicylaldehyde (**7**) in the presence of $ZnCl_2$ to give the Zn(II)-salophen functionalized resorcin[4]arene **Zn-cav**. Unfortunately, the high solubility of the final complex **Zn-cav** did not allow to collect it by simple filtration from the reaction media. This feature had usually facilitated the isolation and purification of analogous salophen derivatives. The pure compound **Zn-cav** was obtained by re-crystallization from acetonitrile in a 74% yield.

The ^{1}H NMR of **Zn-cav** in DMSO-d_6 displayed sharp signals consistent in number with a C_s symmetry (Figure 3).

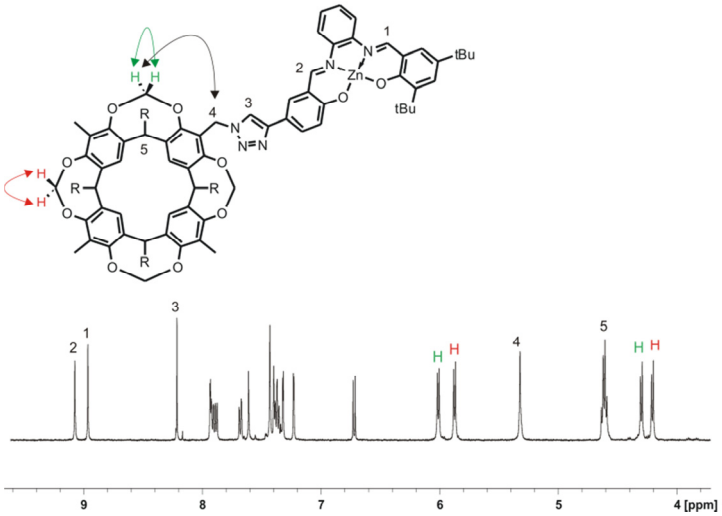

Figure 3. ^{1}H NMR of **Zn-cav** in DMSO-d_6.

The two different iminic protons at 9.07 ppm and 8.96 ppm proved the non-symmetric substitution of the Zn(II)-salophen. The correct functionalization of the resorcin[4]arene with the Zn(II)-salophen was confirmed by the presence of the proton belonging to the 1,2,3-triazole ring as a sharp singlet at 8.21 ppm.

There are two CH_2 bridging units in the resorcin[4]arene macrocicle that are chemically non-equivalent and each one contains two protons also chemically non-equivalent. Thus, the methylene bridging protons resonated as two sets of two doublets.[27] The protons signals of the methylene bridges could be easily assigned by means of 2D NOESY and HSQC analysis. In the NOESY spectrum (Figure 4, a), the NOE cross peaks observed for one set of doublets of one methylene bridge with the benzylic protons allowed the assignment of the two different methylene groups (see green and red in Figure 3). The two carbons of the bridges appeared as two separated singlets in the ^{13}C NMR (97.25 and 97.89 ppm) and by HSQC we could confirm the chemically non equivalent nature of the CH_2 protons in two chemically non equivalent bridges (Figure 4, b).

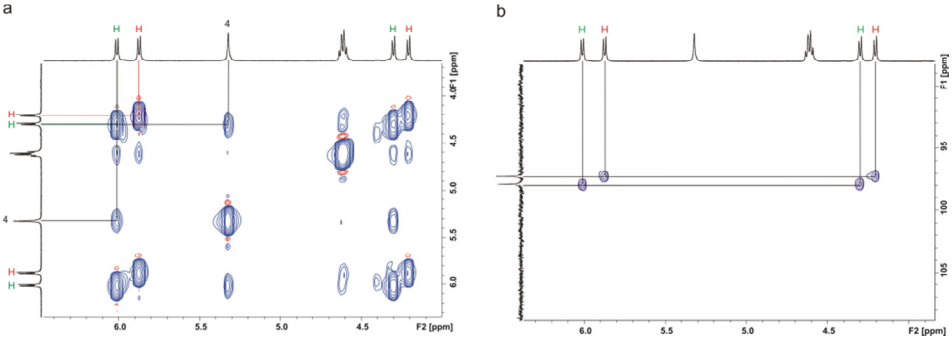

Figure 4. 2D NMR experiments used for the assignment of the protons of the methylene bridges of **Zn-cav**. a: selected region of the NOESY spectrum; b: selected region of the ^{1}H ^{13}C HSQC spectrum.

Crystals suitable for X-Rays analysis grew from acetonitrile solution and demonstrated the strong tendency of the Zn(II)-salophen unit to dimerize through axial oxygen coordination with adjacent molecules, even in the presence of a coordinating solvent (Figure 5). This tendency is well known and could be observed both in solution and in the solid state especially when bulky groups (*e.g. t*-Bu groups) in the 3,3′-position were absent.[28,29] In our case the presence of a *t*-Bu group in only one of the 3-positions of the ligand skeleton was not enough to prevent the formation of dimers in the solid state.

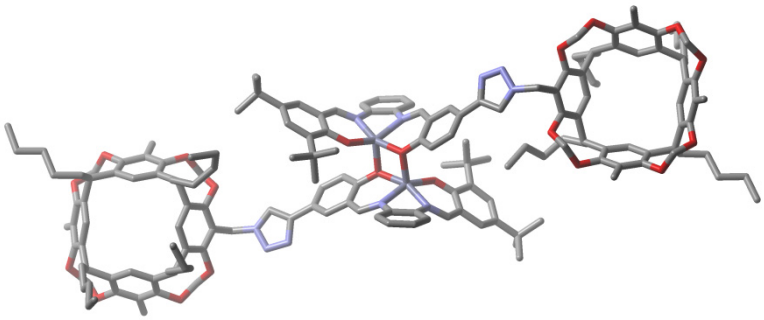

Figure 5. X-Ray structure of (**Zn-cav**)$_2$.

The existence of **Zn-cav** in its dimeric form could be also detected in the gas-phase. The MALDI-TOF spectra of **Zn-cav** showed the ion peaks for both the monomer (*m*/*z* 1429.9) and the dimer (*m*/*z* 2860.8) displaying a perfect fit between experimental and theoretical isotopic patterns.

3.2.2 Binding studies

Before starting the kinetic studies, we tested the binding of PNPCC to receptor **Zn-cav**. From molecular modeling studies, we could estimate that the distance between the resocinarene cavity and the zinc metal center was appropriate to allow the simultaneous cation-π interaction of the ammonium group with the electron rich cavity, and the axial coordination of the carbonyl oxygen with the Zn(II) metal of the salophen unit, (Figure 6).

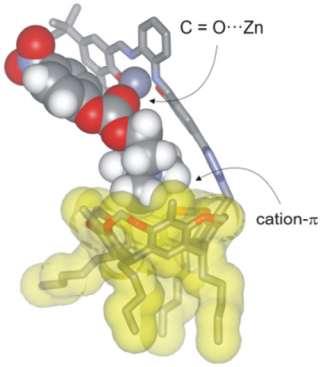

Figure 6. Energy-minimized complex **Zn-cav·PNPCC**

However, during the NMR titration in CD_2Cl_2/MeOD 99:1 the PNPCC was easily hydrolyzed by **Zn-cav**, rendering the analysis of the spectra much more complicated. To overcome this problem, we chose Acetylcholine (**ACh**) as a suitable model for PNPCC. Acetylcholine is hydrolyzed much slower under these conditions and possesses an analogous ammonium knob that can be recognized by the resorcinarene binding site. Moreover the carbonyl group is located at the same distance of the trimethylammonium groups than in PNPCC. When 1 equivalent of **ACh** was added to a solution of **Zn-cav** in CD_2Cl_2/MeOD 95:5, the protons belonging to the trimethylammonium groups in the **ACh** experienced a reduced shielding effect (Figure 7). The signals corresponding to the methyl groups of the **ACh** were upfield shifted ($\Delta\delta$ = -0.1 ppm) with respect to free **ACh**. This is indicative of the binding of the trimethylammonium groups of **ACh** into the aromatic cavity of **Zn-cav**. The binding equilibrium is fast on the NMR timescale and the binding constant of the formed complex is too low to be measured accurately.

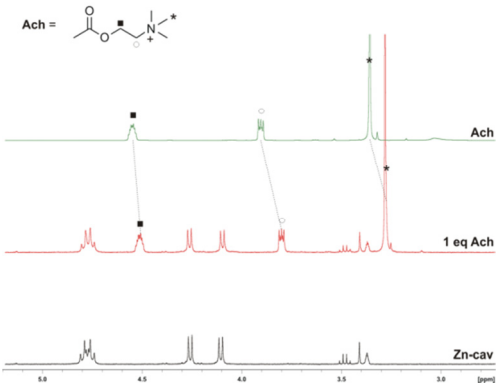

Figure 7. ^{1}H NMR spectra of **Zn-cav** in CD_2Cl_2/MeOD 95:5 upon addition of **ACh**.

3.2.3 Kinetic studies

Kinetic studies of the hydrolysis of the PNPCC (as iodide salt) were performed in CH_2Cl_2 solution under basic conditions, according to already reported

procedures.[17,18] As stated by Rebek, the hydrolysis was carried out by the water present in the commercial CH_2Cl_2[18,30] and was expected to give choline, CO_2, and the *p*-nitrophenolate anion (Scheme 3), which formation could be easily followed by UV-vis absorption measurements (λ = 405 nm).

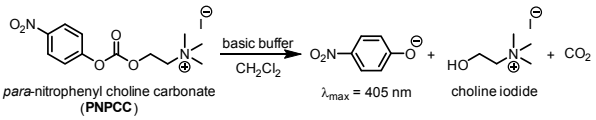

Scheme 3. Hydrolysis reaction of **PNPCC**.

In Figure 8 the experimental kinetics curves obtained using different additives are presented. The reaction is known to proceed through a first order reaction model.[17,18,21]

The rate constant values (k_{obs}) calculated from the initial reaction rate are summarized in Table 1 and are consistent with the previously reported ones.[18]

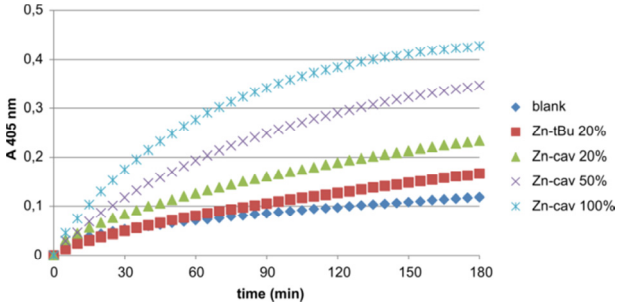

Figure 8. Plots of the absorbance at 405 nm versus time, at different concentration of catalyst.

In the presence of a basic buffer, but in the absence of any catalyst, the reaction is quite slow (entry 1), and after 3 hours only 25% of the starting material is hydrolyzed. The addition of **Zn-cav** caused a moderate increase in the reaction rate constant, which is increased almost four-fold when stoichiometrically amount of **Zn-cav** was used as catalyst (entries 1-4). Symmetrically substituted Zn-salophen derivative with *t*-butyl groups, **Zn-tBu**, was used as a model compound since it could simulate the potential catalytic site (*i.e.* the zinc Lewis

acid) without having the recognition moiety, (*i.e.* the resorcin[4]arene macrocycle). In the presence of 20% of **Zn-tBu**, the increase measured in the reaction rate constant is smaller than the one observed adding the same amount of **Zn-cav** (compare entry 5 with entry 2).

Table 1. Effect of different additives on the rate of the hydrolysis of PNPCC. [a]

entry	catalyst (mole %)	$k_{obs} \times 10^{-3} mn^{-1}$[b]	k_{obs}/k_0[c]
1	-	1.3	1
2	**Zn-cav** (20)	2.3	1.8
3	**Zn-cav** (50)	3.3	2.5
4	**Zn-cav** (100)	5.0	3.8
5	**Zn-tBu** (20)	1.7	1.3

[a] Conditions: 40 μM PNPCC, 20 mM DIPEA/0.5 mM TFA buffer in CH_2Cl_2 at 25°C. [b] Standard errors ±10%. [c] Background hydrolysis.

Carbonate **2**, lacking the ammonium group, is supposed not to be bound by the resorcinarene cavity. Its hydrolysis, in fact, proceeded with the identical rate constant in the presence of the two potential catalysts **Zn-cav** or **Zn-tBu**. This result indicated that the cavity of the **Zn-cav** plays no role when carbonate **2** is used as a substrate. In this case only the zinc metal center is responsible for the observed catalysis.

Further confirmation of this finding derived from the absence of catalysis when cavitand **1** was used as catalyst. The zinc metal center of the salophen is clearly the catalytic center.

3.3 Conclusions

In this project we designed and prepared a novel resorcin[4]arene derivative, **Zn-cav**, functionalized with a Zn(II)-salophen unit. This molecule, shallower and more flexible than similar resorcin[4]arene derivatives, was exploited as

catalyst in the hydrolysis of **PNPCC**. The catalysis observed was not very high compared to the one observed with a model compound (**Zn-tBu**). This result can be explained considering that the binding constant between **Zn-cav** and **PNPCC** is low and consequently there is little amount of **Zn-cav·PNPCC** complex in solution in the experimental conditions. To overcome this problem, future studies will be devoted to the modification of the resorcin[4]arene macrocycle through the insertion of aromatic walls in order to create a deeper cavitand.

3.4 Experimental section

Methyl-resorcin[4]arene[31], bridgded methyl-resorcin[4]arene **1**[32], monobromo bridged resorcin[4]arene **3**[32] and PNPCC[33] were prepared according to reported procedures. 5-ethynyl-2-hydroxybenzaldehyde **5** was prepared as described in Chapter 4.

Synthesis of 4. The monobrominated resorcinarene **3** (0.3 g, 0.32 mmol) was solubilized in 3 mL of dry DMF and NaN_3 (0.03 g, 0.47 mmol) was added. The reaction was stirred overnight at room temperature. The day after a white precipitate was formed. The reaction mixture was poured into water at 0º C and the white precipitate was collected upon filtration and dried. Yield: 87%.

^{1}H NMR (500 MHz, $CDCl_3$) δ 7.19 (s, 1H), 6.99 (m, 3H), 5.94 (d, *J* = 7.0 Hz, 2H), 5.89 (d, *J* = 7.0 Hz, 2H), 4.78 (dt, *J* = 16.5, 8.1 Hz, 4H), 4.56 (s, 2H), 4.40 (d, *J* = 7.0 Hz, 2H), 4.28 (d, *J* = 7.0 Hz, 2H), 2.29 – 2.14 (m, 8H), 2.05 (s, 3H), 1.98 (s, 6H), 1.50– 1.29 (m, 24H), 0.94 (t, *J* = 7.2 Hz, 12H).

^{13}C NMR (125 MHz, $CDCl_3$) δ 153.53, 153.44, 153.28, 153.20, 138.53, 138.14, 137.76, 137.15, 123.99, 123.90, 122.09, 121.40, 117.28, 117.15, 99.43, 98.26, 45.55, 36.99, 36.94, 32.06, 32.00, 31.94, 30.13, 30.00, 27.64, 27.59, 22.67, 22.60, 14.10, 14.08, 10.49, 10.16.

HRMS-ESI+ *calc* for [M+Na$^+$]: 936.5133, found: 936.5147.

Synthesis of 6. Azidomethyl-resorcinarene **4** (183 mg, 0.2 mmol), 5-ethynyl-2-hydroxybenzaldehyde **5** (29 mg, 0.2 mmol), [Cu(CH3CN)$_4$]PF$_6$ (37 mg, 0.1 mmol) and tris((1-benzyl-1H-1,2,3-triazol-4-yl)methyl)amine (11 mg, 0.02 mmol) were solubilized in DMF and stirred at room temperature for 2h. The reaction mixture was diluted with EtOAc and washed with saturate solution of ammonium chloride. The organic layer was died over Na_2SO_4 and the solvent was removed under reduced pressure. The crude was solubilized in a minimal amount of DCM and purified by column chromatography (Hex/AcOEt 2:1). Yield 75%.

^{1}H NMR (500 MHz, $CDCl_3$) δ 11.06 (s, 1H), 9.96 (s, 1H), 8.02 (d, *J* = 2.2 Hz, 1H), 7.92 – 7.84 (m, 2H), 7.24 (s, 1H), 7.07 (d, *J* = 8.6 Hz, 1H), 6.98 (m, 3H), 5.84 (d, *J* = 7.0 Hz, 2H), 5.68 (d, *J* = 7.0 Hz, 2H), 5.44 (s, 2H), 4.75 (dt, *J* = 16.5, 8.1 Hz, 4H), 4.45 (d, *J* = 7.0 Hz, 2H), 4.05 (d, *J* = 7.0 Hz, 2H), 2.29 – 2.14 (m, 8H), 2.04 (s, 3H), 1.87 (s, 6H), 1.48 – 1.28 (m, 24H), 0.91 (m, 12H).

^{13}C NMR (125 MHz, $CDCl_3$) δ 196.41, 161.61, 153.82, 153.55, 153.37, 153.13, 146.05, 138.40, 138.26, 137.71, 136.75, 134.07, 130.52, 124.03, 123.87, 122.48, 122.29, 120.72, 120.03, 119.66, 118.43, 117.13, 117.10, 99.45, 98.32, 44.48, 37.01, 36.98, 32.07, 32.02, 30.19, 30.16, 27.66, 27.63, 22.69, 14.10, 10.46, 10.32.

HRMS-ESI+ *calc* for [M+Na$^+$]: 1082.5501, found: 1082.5459.

Synthesis of Zn-cav. Salicylaldehyde **6** (0.1 g, 0.09 mmol) and the monoimine **7** (0.03 g, 0.09 mmol) were solubilised in 2 mL of DCM. $ZnCl_2$ (14 mg, 0.1 mmol) was solubilized in 1 mL of MeOH and added to the reaction mixture. Lastly, 30 μL of Et_3N were added. The reaction was stirred 2 hours and the solvent was evaporated. The crude was solubilized in AcCN and the yellow precipitate that forms upon slow evaporation was filtered and dried. Yield: 74%.

^{1}H NMR (500 MHz, DMSO-d_6) δ 9.08 (s, 1H), 8.98 (s, 1H), 8.22 (s, 1H), 7.97 – 7.86 (m, 3H), 7.69 (dd, *J* = 8.8, 2.4 Hz, 1H), 7.62 (s, 1H), 7.44 (s, 2H), 7.43 – 7.31 (m, 4H), 7.24 (d, *J* = 2.7 Hz, 1H), 6.72 – 6.74 (d, 1H), 6.02 (d, *J* = 7.6 Hz, 2H), 5.88 (d, *J* = 7.6 Hz, 2H), 5.33 (s, 2H), 4.62 (dt, *J* = 8.0 Hz, 4H), 4.31 (d, *J* = 7.6 Hz, 2H), 4.22 (d, *J* = 7.6 Hz, 2H), 2.48 – 2.20 (m, 8H), 1.92 – 1.91 (s, 6H), 1.91 – 1.90 (s, 3H), 1.50 (s, 9H), 1.45 – 1.35 (m, 8H), 1.35 – 1.26 (m, 25H), 0.87 (td, *J* = 7.2, 6.1 Hz, 12H).

^{13}C NMR (125 MHz, DMSO) δ 171.14, 169.55, 162.78, 161.53, 152.05, 151.81, 151.70, 151.61, 145.54, 139.80, 139.29, 138.25, 137.59, 137.12, 136.90, 136.26, 132.49, 131.66, 130.88, 128.79, 127.66, 126.58, 125.77, 122.97, 122.86, 122.81, 122.13, 120.84, 118.91, 118.46, 118.17, 117.31, 115.68, 115.59, 114.83, 97.88, 97.24, 42.63, 36.10, 36.05, 34.34, 32.71, 30.64, 30.50, 28.79, 28.38, 28.32, 26.59, 26.56, 21.45, 21.41, 13.11, 9.15.

HRMS-ESI+ *calc* for [M+Na$^+$]: 1450.6732, found: 1450.6736.

3.5 NMR Spectra

^{1}H NMR (500 MHz, $CDCl_3$) of compound **6**

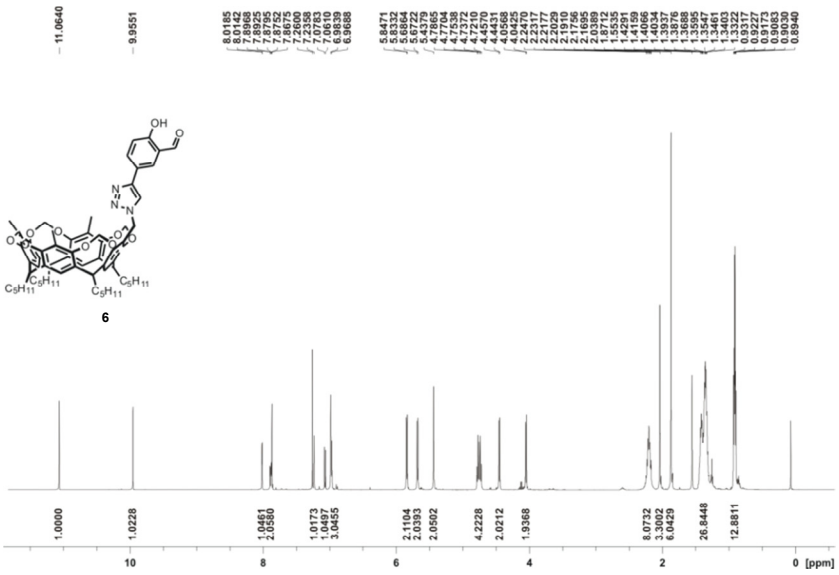

^{13}C NMR (125 MHz, $CDCl_3$) of compound **6**

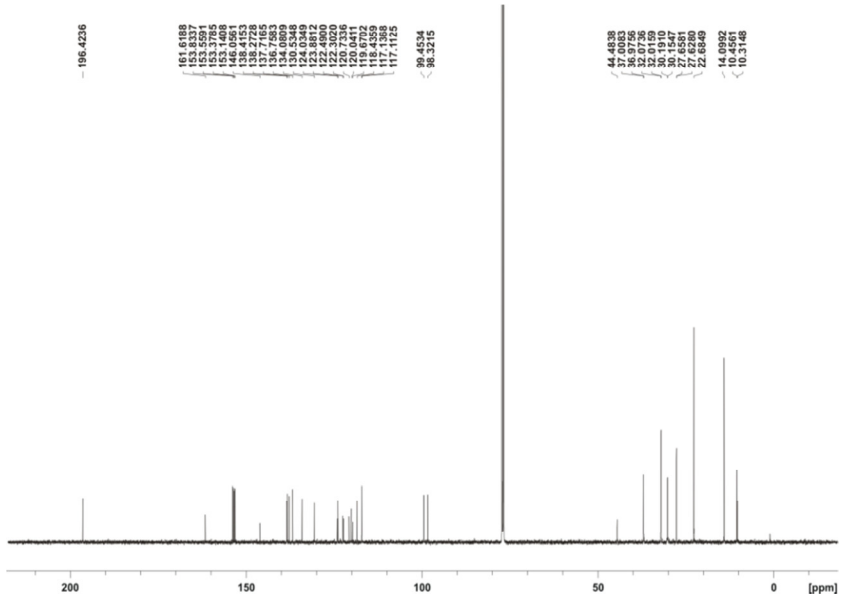

^{1}H NMR (500 MHz, DMSO-d_6) of compound **Zn-cav**

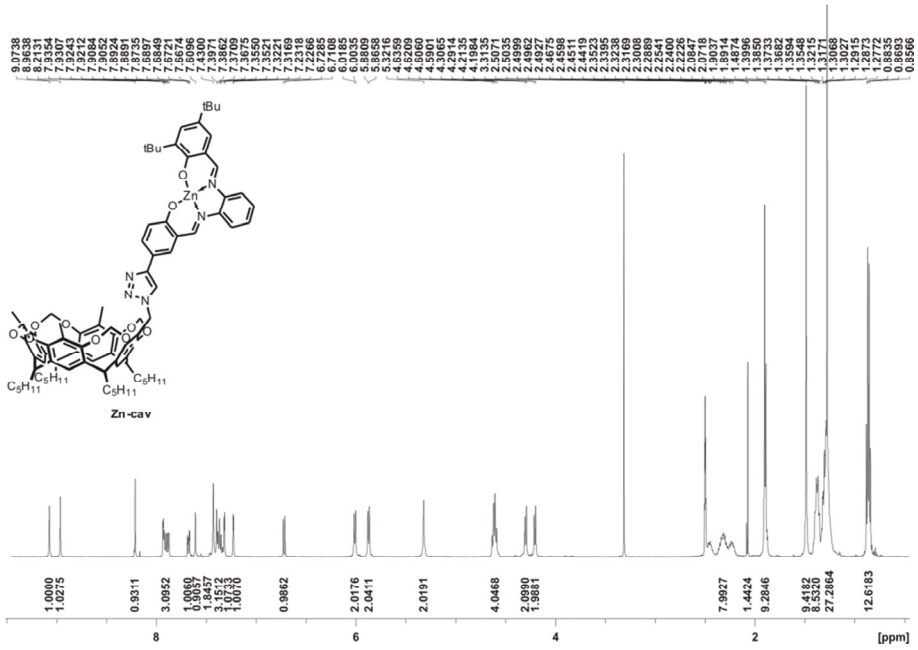

^{13}C NMR (125 MHz, DMSO) of compound **Zn-cav**

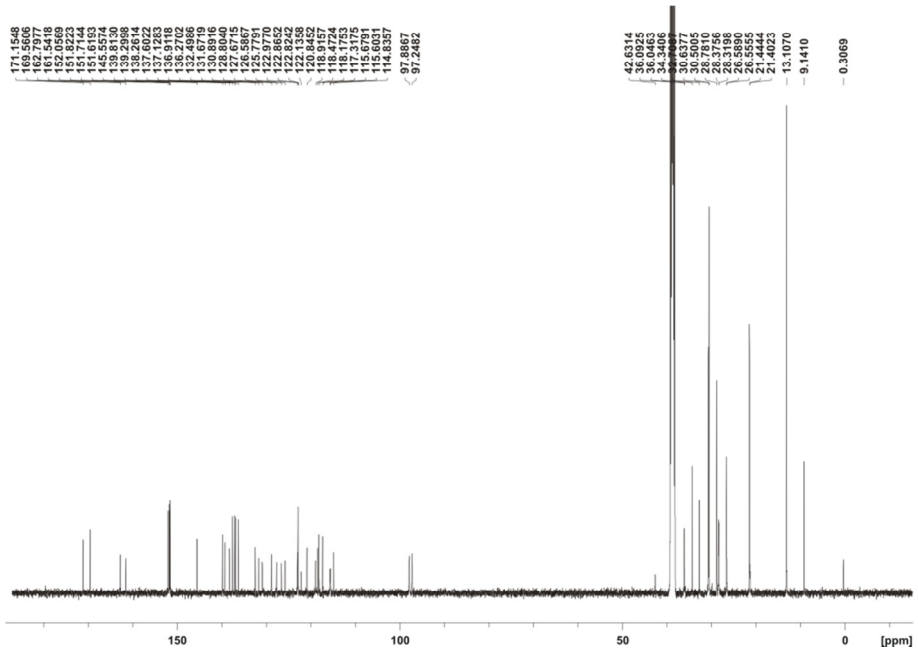

3.6 References

[1] M. Raynal, P. Ballester, A. Vidal-Ferran, P. W. N. M. van Leeuwen, *Chem. Soc. Rev.* **2014**, *43*, 1660-1733.
[2] M. Raynal, P. Ballester, A. Vidal-Ferran, P. W. N. M. van Leeuwen, *Chem. Soc. Rev.* **2014**, *43*, 1734-1787.
[3] Z. Y. Dong, Q. Luo, J. Q. Liu, *Chem. Soc. Rev.* **2012**, *41*, 7890-7908.
[4] J. Meeuwissen, J. N. H. Reek, *Nature Chemistry* **2010**, *2*, 615-621.
[5] Y. H. Lin, J. S. Ren, X. G. Qu, *Acc. Chem. Res.* **2014**, *47*, 1097-1105.
[6] D. A. Leigh, V. Marcos, M. R. Wilson, *Acs Catalysis* **2014**, *4*, 4490-4497.
[7] P. Thordarson, E. J. A. Bijsterveld, A. E. Rowan, R. J. M. Nolte, *Nature* **2003**, *424*, 915-918.
[8] R. R. Knowles, E. N. Jacobsen, *Proc. Natl. Acad. Sci. U. S. A.* **2010**, *107*, 20678-20685.
[9] R. J. Hooley, J. Rebek, *Chem. Biol.* **2009**, *16*, 255-264.
[10] J. N. Rebilly, B. Colasson, O. Bistri, D. Over, O. Reinaud, *Chem. Soc. Rev.* **2015**, *44*, 467-489.
[11] A. G. S. Högberg, *J. Org. Chem.* **1980**, *45*, 4498–4500.
[12] A. G. S. Hogberg, *J. Am. Chem. Soc.* **1980**, *102*, 6046-6050.
[13] P. Timmerman, W. Verboom, D. N. Reinhoudt, *Tetrahedron* **1996**, *52*, 2663-2704.
[14] S. M. Biros, J. Rebek, *Chem. Soc. Rev.* **2007**, *36*, 93-104.
[15] S. X. Xiao, D. Ajami, J. Rebek, *Org. Lett.* **2009**, *11*, 3163-3165.
[16] B. W. Purse, J. Rebek, *Proc. Natl. Acad. Sci. U. S. A.* **2005**, *102*, 10777-10782.
[17] F. Cuevas, S. Di Stefano, J. O. Magrans, P. Prados, L. Mandolini, J. de Mendoza, *Chem. Eur. J.* **2000**, *6*, 3228-3234.
[18] S. Richeter, J. Rebek, *J. Am. Chem. Soc.* **2004**, *126*, 16280-16281.
[19] A. Gissot, J. Rebek, *J. Am. Chem. Soc.* **2004**, *126*, 7424-7425.
[20] F. H. Zelder, J. Rebek, *Chem. Commun.* **2006**, 753-754.
[21] B. Soberats, E. Sanna, G. Martorell, C. Rotger, A. Costat, *Org. Lett.* **2014**, *16*, 840-843.
[22] P. Ballester, A. Shivanyuk, A. R. Far, J. Rebek, *J. Am. Chem. Soc.* **2002**, *124*, 14014-14016.
[23] A. S. Mahadevi, G. N. Sastry, *Chemical Reviews* **2013**, *113*, 2100-2138.
[24] M. Kokkinidis, N. M. Glykos, V. E. Fadouloglou, *Structural and Mechanistic Enzymology: Bringing Together Experiments and Computing* **2012**, *87*, 181-218.
[25] R. Z. Wu, T. F. Al-Azemi, K. S. Bisht, *Chem. Commun.* **2009**, 1822-1824.
[26] T. F. Al-Azemi, M. Vinodh, *Tetrahedron* **2011**, *67*, 2585-2590.
[27] S. Simaan, S. E. Biali, *J. Phys. Org. Chem.* **2004**, *17*, 752-759.
[28] A. W. Kleij, M. Kuil, M. Lutz, D. M. Tooke, A. L. Spek, P. C. J. Kamer, P. W. N. M. van Leeuwen, J. N. H. Reek, *Inorg. Chim. Acta* **2006**, *359*, 1807-1814.
[29] M. M. Belmonte, S. J. Wezenberg, R. M. Haak, D. Anselmo, E. C. Escudero-Adan, J. Benet-Buchholz, A. W. Kleij, *Dalton Trans.* **2010**, *39*, 4541-4550.
[30] Water present in commercial CH_2Cl_2 measured with Karl Fischer coulometer to be 53 ppm (0.005%). Saturation of CH_2Cl_2 doesn't cause any noticeable changes
[31] D. J. Cram, S. Karbach, H. E. Kim, C. B. Knobler, E. F. Maverick, J. L. Ericson, R. C. Helgeson, *J. Am. Chem. Soc.* **1988**, *110*, 2229-2237.
[32] T. F. Al-Azemi, M. Vinodh, *Tetrahedron* **2011**, *67*, 2585-2590.

[33] A. Gissot, J. Rebek, *J. Am. Chem. Soc.* **2004**, *126*, 7424-7425.

Chapter 4

Application of Zn(II)-salophen in the formation of supramolecular gels

4.1 Introduction

Gels are well known materials that as stated by Dr. Dorothy Jordan Lloyd in 1926 "are easier to recognize than to define".[1]

Gels find numerous applications in our everyday life, such as pharmaceutics, cosmetics and food industries among all, Figure 1.

Figure 1. Scheme showing the different applications of gels in our everyday life.

Typically, they are composed of 99% liquid and only 1% of solid, this latter known as gelator. Despite this composition they have a "solid like" behavior. A gel can be easily recognized because of its flow characteristics, imparted by a three-dimentional fibrillar network. In this 3D network the molecules of solvent are entrapped by capillary forces that prevent its flow.[2,3]

Despite many commercial gels derived from polimers, nowadays, there is growing interest in gels obtained from low-molecular-weight gelators (LMWGs) that self-assembly through specific non-covalent interactions such as hydrogen bonding, π-π stacking, electrostatic and van der Walls ones.[4,5,6,7,8]

The field of supramolecular gels has increased enormously in the last decades. This can be seen as a consequence of the progresses in the field of supramolecular chemistry and in the related self-assembly processes that allowed the control of the gelation properties. Another important factor to consider is the development of analytical methods to understand the gel structure, mainly electron microscopy and NMR methods that are commonly used in the majority of the laboratories.[3]

Gels are generally obtained after solubilization of the gelator in a hot solvent followed by slow cooling at a given temperature.[9] The intrinsic reversible nature of supramolecular gels and the ease to control the sol-gel transition, render them excellent candidates in many different hi-tech applications spreading from biomaterials to electronic devices.[3,10] Some interesting examples reported in the literature regard the use of gels as media for organic reactions[9,11] and crystal growth.[12,13] The introduction of specific functionalities on the molecular gelator, able to respond to physical (*e.g.* temperature, light or sonication) or chemical stimuli allows the tuning of the gel properties upon application of the chosen stimulus.[2,14] The most commonly used chemical stimuli are the variation of pH, changes in the oxidation state, addition of ions or neutral species, incorporation of metals and enzymes.[2,15,16,17,18,19] In particular, anion responsive gels can be prepared introducing anion binding sites such as hydrogen bond donors like amides and ureas.[20]

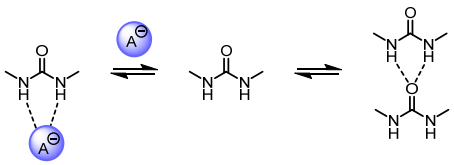

Scheme 1. Competition between gel formation and binding of the anion of a urea derived gelator.

The binding of the anion to the gelator can compete with the gelator self-assembly and cause the gel-sol transition (Scheme 1).[2,17,21]

However, there are cases where the addition of an anion induces a variation in the strength of the gel (*i.e.* weakening or strengthening).[17,21] Gel properties affected by anion binding are generally the rheology, *i.e.* flow characteristics, morphology, but also absorption or fluorescence.

The ability of Zn(II)-salophen to behave as Lewis acids and strongly coordinate in the apical position Lewis bases such as anions and amines is well documented.[22] The binding event is generally followed by changes in absorption or emission. The five-coordinate zinc metal center also promotes the formation of dimers through the coordination of the zinc atom of a salophen to the phenoxy oxygen of another, as already discussed in Chapter 1, Figure 10.[23] MacLachlan and co-workers demonstrated the capacity of Zn(II)-salophens in Figure 2 to form 1D nanofibers and gels upon Zn···O interactions.[24,25]

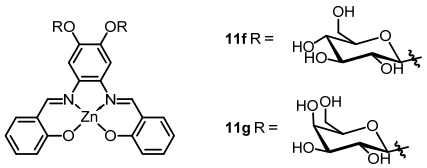

11a R = CH_3
11b R = C_6H_{13}
11c R = 2-ethylhexyl
11d R = $C_{14}H_{29}$
11e R = $C_{16}H_{33}$

Figure 2. Molecules studied by MacLachlan and co-workers.

More recently Olivieri *et al.* reported the formation of nanofibers upon self-assembly of Zn(II)-salophen having alkoxy substituents as lateral groups. They also investigated the effect of different solvents on the aggregation properties of these Zn(II)-salphen complexes and on the fibers morphology.[26,27] Surprisingly, the response of these supramolecular assemblies to the addition of suitable

donor ligands that can coordinate to the Zn(II) metal center is almost unexplored.

In this study, we aimed to investigate the gelation properties of a Zn(II)-salophen functionalized with a small peptide known to act as a gelator and its response to anions and neutral guests. The addition of an anion to a gel most commonly caused the disruption of the gel but also cases where the weakening or strengthening of the gel occurred have been reported.[17,21]

In collaboration with Prof. Beatriu Escuder (Universitat Jaume I, Castelló, Spain) we designed and prepared two peptide functionalized Zn(II)-salohpens, **1a** and **1b** (Figure 3) and tested their gelation properties in different solvents.

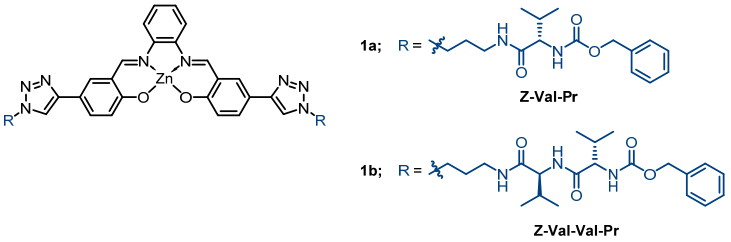

Figure 3. Line drawing structures of the molecules prepared and studied in this chapter.

L-valine derivatives have been extensively studied by Escuder and co-workers as molecular gelators.[28,29] We expected that the presence of the metal could further assist the molecular gelation and also behave as a binding site for guests species.[15,17]

4.2 Results and Discussion

4.2.1 Design and synthesis of 1a and 1b

Compounds **2** and **3** were prepared by the group of Prof. Escuder and have an azide group that allows the functionalization of the salophen skeleton through 1,2,3-triazole ring junction.

From our side, we dealt with the synthesis of 5-ethynyl-2-hydroxybenzaldehyde **1** through the Sonoghashira coupling reaction between the commercially available 5-bromo-2-hydroxybenzaldehyde and ethynyltrimethylsilane followed by deprotection with tetrabutylammonium fluoride (Scheme 2). Aldehydes **4** and **5**, functionalized with derivatives **Z-Val-Pr** and **Z-Val-Val-Pr** respectively, were obtained through the Copper catalyzed Alkyne-Azide Cycloaddition (CuAAC), also known as "click reaction".

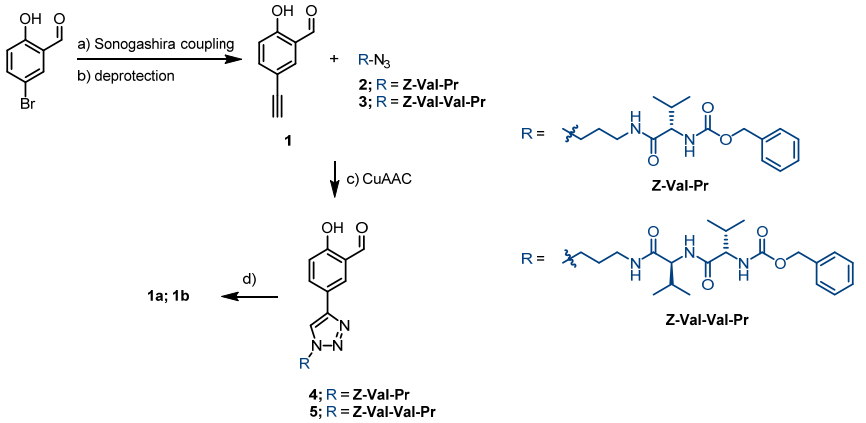

Scheme 2. Synthetic pathway showing the preparation of compounds **1a** and **1b**. Reaction conditions: a) ethynyltrimethylsilane, $Pd(PPh_3)_2Cl_2$, CuI, Et_3N, 80°C, 18 h; b) TBAF 1M in THF, MeOH, room temperature, 1 h; c) $Cu(CH_3CN)_4PF_6$, TBTA, THF/H_2O 1:1, room temperature, 48 h. d) benzene-1,2-diamine, $ZnCl_2$, Et_3N, DCM/MeOH 2:1, r.t., 3-6 h.

The synthesis of the Zn-salophens was accomplished using standard conditions. Contrary, the purification step was slightly modified in order to avoid the loss of material. Generally the product that precipitates in the reaction media is collected upon filtration and washed with cold methanol. In this specific case, however, the tiny solid particles tended to pass through the filter so we decided to recover and purify it through several steps of dissolution/centrifugation. The final compounds were fully characterized

through mono and bi-dimensional NMR techniques and high resolution mass spectra.

4.2.2 Preliminary gelation experiments

With the pure final compounds in hands we started the gelation experiments in different organic solvents. The methodology reported in the literature to obtain a gel, generally involves the dissolution of the solid in the chosen solvent through sonication and/or heating followed by slow cooling. After a certain amount of time (minutes or hours), the tube inversion test is performed. If the solvent does not flow, this means that the gel is formed. This methodology was chosen because of its simplicity and it is well accepted by chemists active in the field.[30]

Gelators derived from L-Valine derivatives are known to gel in solvents as water and acetonitrile,[29] while Zn(II)-salophens forms gels in methanol or in aromatic solvents such as benzene and toluene.[24]

In Table 1 are reported the gelation abilities of **1a** and **1b** in various solvents.

Table 1. Summary of the gelation experiments with **1a** and **1b** in different solvents. Concentration: 3 mg/mL; Y = yes ; N = no.

Solvent	Gelator	Sonication/Temperature	Solubility	Gel
MeOH	**1a**	Y	N	N
	1b	Y	N	N
EtOH	**1a**	Y	N	N
	1b	Y	N	N
Toluene	**1a**	Y	N	N
	1b	Y	N	N
DMF	**1a**	Y	Y	N
	1b	Y	Y	N
Pyridine	**1a**	Y	Y	N
	1b	Y	Y	N
EtOAc	**1a**	Y	N	N
	1b	Y	N	N
THF	**1a**	Y	N	N
	1b	Y	N	N
DCM	**1a**	Y	N	N
	1b	Y	N	N
$CHCl_3$	**1a**	Y	N	N
	1b	Y	N	N
ACN	**1a**	Y	N	N
	1b	Y	N	N
H_2O	**1a**	Y	N	N
	1b	Y	N	N

As can be evidenced in Table 1, none of the solvent tested was gelated by **1a** neither **1b**. This result could be ascribed to the low solubility of both the compounds in the majority of the solvent tested. On the other hand, coordinating solvents such as dimethyl sulfoxide (DMSO), pyridine or N,N-dimethylformamide (DMF) where both **1a** and **1b** are soluble, prevented the

formation of gels. For these reasons we decided to prior dissolve **1a** and **1b** in a small amount of DMSO and than add the other solvent. In Table 2 are summarized the results obtained with this second technique. Now, both **1a** and **1b** are soluble in toluene and tetrahydrofuran (THF) while only **1b** resulted soluble in chloroform ($CHCl_3$) and acetonitrile (ACN). Furthermore, **1b** was able to gelate acetonitrile as can be seen in Figure 4. The gel formed instantaneously after the addition of few drops of acetonitrile to a concentrated solution of **1b** in DMSO, without sonication or heating.

Table 2. Gelation experiments with **1a** and **1b** dissolved in a small amount of DMSO.

Solvent	Gelator	Sonication/Temperature	Solubility	Gel
MeOH	**1a**	Y	N	N
	1b	Y	N	N
EtOH	**1a**	Y	N	N
	1b	Y	N	N
Toluene	**1a**	Y	Y	N
	1b	Y	Y	N
EtOAc	**1a**	Y	N	N
	1b	Y	N	N
THF	**1a**	Y	Y	N
	1b	Y	Y	N
DCM	**1a**	Y	N	N
	1b	Y	N	N
$CHCl_3$	**1a**	Y	N	N
	1b	Y	Y	N
ACN	**1a**	Y	N	N
	1b	N	Y	Y
H_2O	**1a**	Y	N	N
	1b	Y	N	N

However, the formation of this gel does not seem to be reversible and after dissolution of the gel upon sonication and heating we were not able to obtain the gel again.

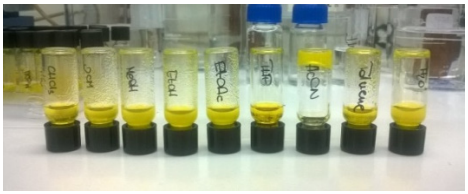

Figure 4. Picture of the tube inversion tests with gelator **1b** previously dissolved in DMSO.

The presence of aggregates was also evidenced in the gas phase. MALDI spectra of the complex **1b** show the peak corresponding to the molecular ion with the expected isotopic pattern, but also revealed the existence of aggregates up to five units of monomers (Figure 5)

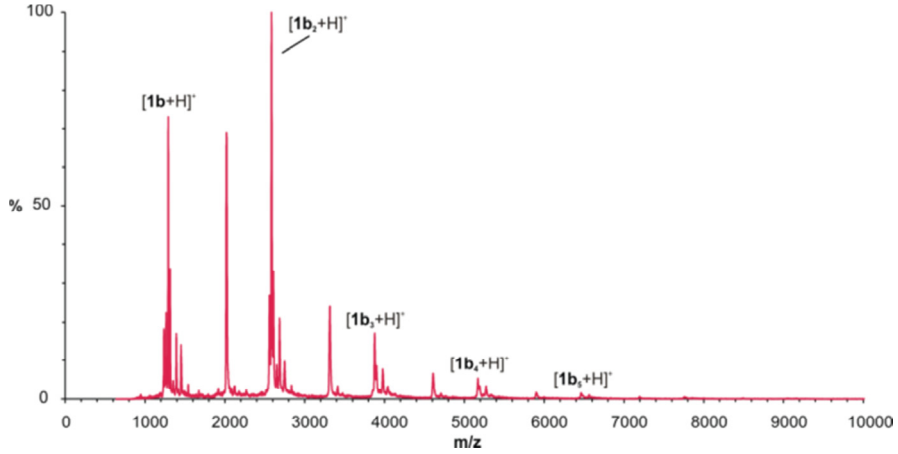

Figure 5. MALDI spectrum of compound **1b**.

4.2.3 Effect of a guest addition on the formation of the gel

As stated before, Zn(II)-salophen complexes are good receptors for tertiary amines and anions.[22] In order to evaluate the effect of the addition of neutral species or anions on gel formation, we dissolved 2-3 equivalents of a chosen guest in acetonitrile before adding it to the gelator **1b** in DMSO. In all the cases,

the gel did not form instantaneously as when pure acetonitrile was added. However, after few minutes, the solutions containing 1,4-diazabicyclo[2.2.2]octane, (DABCO) tetrabutylammonium chloride, tetrabutylammonium acetate and quinuclidine became cloudy and the gel formed as can be seen in Figure 6.

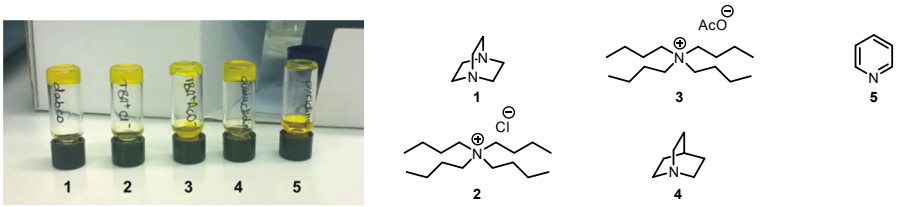

Figure 6. Photograph of the gelation tests with gelator **1b** in DMSO/ACN in the presence of different guests.

In the presence of tetrabutylammonium acetate the gel was not strong enough and was easily broken during the tube inversion test. Few equivalents of pyridine were instead able to prevent the gel formation. These preliminary results suggested that both the basicity and the size of the guest are important factors in the formation of the gel. In fact, we could assume the existence of a double contribution that govern gelation ability *i.e.* the intermolecular Zn···O interactions as observed by MacLachlan and co-workers[24,25] and multiple hydrogen bonds between **Z-Val-Val-Pr** residues as already described for similar LMWGs gelators.[8] The evidence that the gel is still formed when small guests that coordinate to the zinc are present can be an indication of the fact that the major contribution for gel formation arose from the H-bond network created by the L-valine derivatives as schematically illustrated in Figure 7.

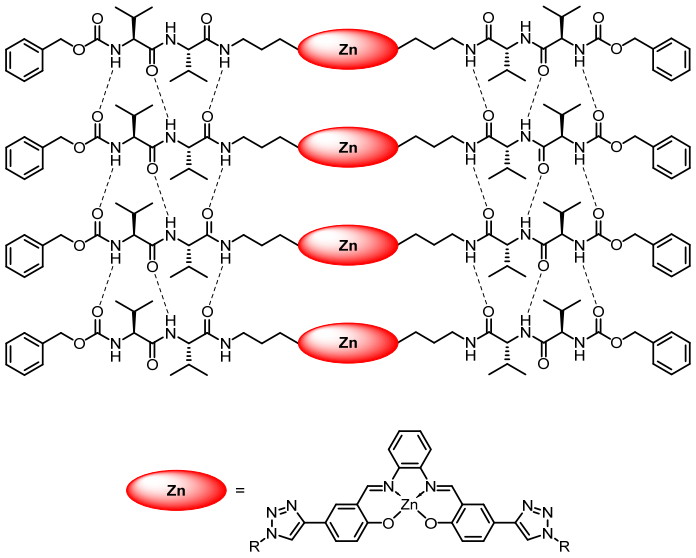

Figure 7. Schematic representation for the proposed aggregation mode of compound **1b**.

4.3 Conclusions

The synthesis of two different Zn(II)-salophens functionalized with gelators **Z-Val-Pr** and **Z-Val-Val-Pr** was successfully accomplished. Preliminary gelation tests revealed the capability of salophen **1b** to gelate acetonitrile when previously dissolved in DMSO. Finally, we investigated the behavior of the gel in the presence of different guests. In the presence of DABCO, tetrabutylammonium chloride and quinuclidine the gel was still formed, suggesting that the zinc metal center is not involved in the formation of the gel network. Further insights into the gel properties will be carried out in collaboration with Prof. Escuder in the next future.

4.4 Experimental section

Synthesis of 2-hydroxy-5-((trimethylsilyl)ethynyl)benzaldehyde. 5-bromo-2-hydroxybenzaldehyde (0.5 g, 2.5 mmol), $Pd(PPh_3)_2Cl_2$ (52 mg, 0.08 mmol) and

CuI (24 mg, 0.12 mmol) were added in a dry schlenk tube and vacuum/Argon cycles were performed. Dry Et_3N (8 mL) was added and stirred at 80ºC. Lastly, ethynyltrimethylsilane (0.53 mL, 3.73 mmol) was added and the reaction was capped under Argon atmosphere and stirred at 80º for 24h. The reaction was transferred in a round bottom flask and the solvent was evaporated under vacuum. The crude was plugged on silica with EtOAc and then purified on silica column (Hex/EtOAc 99:1). Yield 89%.

^{1}H NMR (500 MHz, $CDCl_3$) δ 11.12 (s, 1H), 9.88 (s, 1H), 7.73 (d, *J* = 2.1 Hz, 1H), 7.63 (dd, *J* = 8.7, 2.1 Hz, 1H), 6.96 (d, *J* = 8.7 Hz, 1H), 0.28 (s, 9H).

^{13}C NMR (125 MHz, $CDCl_3$) δ 196.01, 161.52, 140.14, 137.36, 120.34, 117.96, 115.13, 103.13, 93.82, -0.08.

Synthesis of 5-ethynyl-2-hydroxybenzaldehyde (1). 2-hydroxy-5-((trimethylsilyl)ethynyl)benzaldehyde 0.94 g, 4.3 mmol) was partially solubilized in 15 mL of MeOH and TBAF 1M in THF (15 mL, 15 mmol) was added. The reaction was stirred at room temperature for 2 hours. Then water was added to the reaction mixture and extracted with DCM for three times. The organic layers were combined and dried over Na_2SO_4 and the solvent was evaporated. The crude was purified on silica column (eluent: Hex/EtOAc 95:5). Yield 70%.

^{1}H NMR (300 MHz, $CDCl_3$) δ 11.14 (s, 1H), 9.88 (s, 1H), 7.74 (d, *J* = 2.1 Hz, 1H), 7.64 (dd, *J* = 8.7, 2.1 Hz, 1H), 6.98 (d, *J* = 8.7, 1H), 3.06 (s, 1H).

Synthesis of (S)-benzyl (1-((3-(4-(3-formyl-4-hydroxyphenyl)-1H-1,2,3-triazol-1-yl)propyl)amino)-3-methyl-1-oxobutan-2-yl)carbamate (4). 5-ethynyl-2-hydroxybenzaldehyde (120 mg, 0.82 mmol) was dissolved in 2 mL of THF and a solution of (S)-benzyl (1-((3-azidopropyl)amino)-3-methyl-1-oxobutan-2-yl)carbamate (274 mg, 0.82 mmol) in 2 mL of THF was added. Subsequently $Cu(CH_3CN)_4PF_6$ (15 mg, 0.04 mmol) and TBTA (tris((1-benzyl-1H-1,2,3-triazol-

4-yl)methyl)amine, 13 mg, 0.02 mmol) were added to the reaction mixture. Before capping 2 mL of water were added. The reaction was stirred at room temperature for 48 hours, then diluted with water and extracted with EtOAc. The organic layer was dried over Na_2SO_4 and the solvent was removed under vacuum. The crude was purified on silica (eluent: AcOEt/Hex 9:1). The compound was obtained as a white solid. Yield 50%.

^{1}H NMR (300 MHz, $CDCl_3$) δ 11.07 (s, 1H), 9.98 (s, 1H), 8.13 (d, *J* = 2.2 Hz, 1H), 7.94 (dd, *J* = 8.7, 2.2 Hz, 1H), 7.89 (s, 1H), 7.41 - 7.28 (m, 5H), 7.07 (d, *J* = 8.7 Hz, 1H), 6.30 (m, 1H), 5.28 (m, 1H), 5.12 (s, 2H), 4.48 - 4.37 (m, 2H), 3.95 (dd, *J* = 8.2, 6.1 Hz, 1H), 3.39 - 3.26 (m, 2H), 2.27 - 2.08 (m, 3H), 0.97 (dd, *J* = 15.0, 6.8 Hz, 6H).

^{13}C NMR (125 MHz, $CDCl_3$) δ 196.61, 171.89, 161.41, 156.54, 146.35, 136.07, 134.27, 130.70, 128.57, 128.31, 128.07, 122.94, 120.72, 119.75, 118.23, 67.23, 60.94, 47.49, 36.21, 30.56, 30.24, 29.70, 19.39, 17.84.

HRMS-ESI+ *calc* for [M+Na^+]: 502.2061, found: 502.2054.

Synthesis of 1a. (S)-benzyl (1-((3-(4-(3-formyl-4-hydroxyphenyl)-1H-1,2,3-triazol-1-yl)propyl)amino)-3-methyl-1-oxobutan-2-yl)carbamate (100 mg, 0.2 mmol) was solubilized in 1 mL of DCM and benzene-1,2-diamine (11 mg, 0.1 mmol) in 0.5 mL of DCM was added. $ZnCl_2$ (16 mg, 0.12 mmol) was dissolved in 0.5 mL of MeOH and added to the reaction mixture. Finally 29 μL of Et_3N (0.2 mmol) were added. The reaction was stirred 6 hours at room temperature. The reaction was transferred in an Eppendorf and centrifuged. The liquid was collected, concentrated and centrifuged again. The centrifuged solid was washed with MeOH 2 times and then solubilized with DCM, transferred in a flask and concentrated.

^{1}H NMR (500 MHz, DMSO-d_6) δ 9.13 (s, 2H), 8.30 (s, 2H), 8.14 - 8.08 (m, 2H), 7.99 (d, *J* = 2.4 Hz, 2H), 7.96 (m, 2H), 7.68 (dd, *J* = 8.8, 2.4 Hz, 2H), 7.46 - 7.40 (m,

2H), 7.39 - 7.27 (m, 12H), 6.81 (d, *J* = 8.8 Hz, 2H), 5.04 (s, 4H), 4.40 (t, 4H), 3.80 (t, 2H), 3.20 - 3.07 (m, 4H), 2.06 - 1.91 (m, 6H), 0.88 (dd, *J* = 6.7, 2.2 Hz, 12H).

^{13}C NMR (125 MHz, DMSO) δ 172.52, 171.88, 163.23, 156.65, 147.18, 139.88, 137.50, 133.06, 132.32, 128.78, 128.23, 128.11, 127.98, 124.05, 119.78, 119.67, 117.10, 116.41, 65.88, 61.03, 47.62, 46.26, 36.20, 30.51, 30.29, 19.73, 18.83.

HRMS-MALDI+ *calc* for [M+Na$^+$]: 1115.3841; found: 1115.3873

Synthesis of benzyl ((R)-1-(((R)-1-((3-(4-(3-formyl-4-hydroxyphenyl)-1H-1,2,3-triazol-1-yl)propyl)amino)-3-methyl-1-oxobutan-2-yl)amino)-3-methyl-1-oxobutan-2-yl)carbamate (5). Benzyl ((S)-1-(((S)-1-((3-azidopropyl)amino)-3-methyl-1-oxobutan-2-yl)amino)-3-methyl-1-oxobutan-2-yl)carbamate (76 mg, 0.18 mmol) was solubilized in 1.2 mL of THF and 5-ethynyl-2-hydroxybenzaldehyde (28 mg, 0.19 mmol) was added. Suddenly 0.6 mL of water were added to the reaction mixture. Lastly $Cu(CH_3CN)_4PF_6$ (32 mg, 0.09 mmol) and TBTA (tris((1-benzyl-1H-1,2,3-triazol-4-yl)methyl)amine, 9 mg, 0.018 mol) were added and the reaction was stirred at room temperature overnight. Then was diluted with water and extracted with DCM. The organic layers were combined and dried over Na_2SO_4. The solvent was evaporated and the compound was purified by silica column chromatography (eluent: DCM/MeOH 95:5). Yield 96%.

^{1}H NMR (400 MHz, $CDCl_3$) δ 11.07 (s, 1H), 9.98 (s, 1H), 8.13 (d, *J* = 2.2 Hz, 1H), 7.98 (s, 1H), 7.94 (dd, *J* = 8.7, 2.2 Hz, 1H), 7.40 - 7.30 (m, 5H), 7.06 (d, *J* = 8.7 Hz, 1H), 6.76 - 6.71 (m, 1H), 6.52 (d, *J* = 8.2 Hz, 1H), 5.37 (d, *J* = 6.5 Hz, 1H), 5.16 (d, *J* = 12.3 Hz, 1H), 5.08 (d, *J* = 12.3 Hz, 1H), 4.44 (t, *J* = 6.6 Hz, 2H), 4.28 - 4.20 (m, 1H), 4.03 (t, *J* = 6.1 Hz, 1H), 3.34 (m, 1H), 3.21 (m, 1H), 2.31 - 2.12 (m, 4H), 1.02 (d, *J* = 6.8 Hz, 3H), 0.96 (t, *J* = 6.9 Hz, 6H), 0.85 (d, *J* = 6.8 Hz, 3H).

^{13}C NMR (125 MHz, $CDCl_3$) δ 196.68, 171.65, 171.43, 161.33, 156.94, 146.19, 135.92, 134.29, 130.70, 128.62, 128.57, 128.40, 127.96, 123.07, 120.71, 120.08,

118.16, 67.38, 61.32, 59.02, 47.49, 36.15, 30.39, 30.14, 29.80, 29.70, 19.48, 19.31, 17.88, 17.76.

HRMS-ESI+ *calc* for [M+Na^+]: 601.2738, found: 601.2745.

Synthesis of 1b. Benzyl ((S)-1-(((S)-1-((3-(4-(3-formyl-4-hydroxyphenyl)-1H-1,2,3-triazol-1-yl)propyl)amino)-3-methyl-1-oxobutan-2-yl)amino)-3-methyl-1-oxobutan-2-yl)carbamate (58 mg, 0.1 mmol) was solubilized in 1 mL of DCM and a solution of benzene-1,2-diamine (5.42 mg, 0.05 mmol) in 0.5 mL of MeOH and $ZnCl_2$ (7.51 mg, 0.05 mmol) were added. Finally 14 μL of Et_3N were added and the reaction was stirred 3 hours at room temperature. Then, the reaction was transferred in an Eppendorf and centrifuged. The solvent was removed and the solid was washed with DCM and MeOH. Yield 40%.

^{1}H NMR (500 MHz, DMSO-d_6) δ 9.13 (s, 2H), 8.30 (s, 2H), 8.17 – 8.12 (m, 2H), 7.99 (d, *J* = 2.5 Hz, 2H), 7.96 (dd, *J* = 6.2, 3.5 Hz, 2H), 7.75 (d, *J* = 8.6 Hz, 2H), 7.68 (dd, *J* = 8.8, 2.5 Hz, 2H), 7.42 (dd, *J* = 6.2, 3.5 Hz, 2H), 7.40 – 7.29 (m, 12H), 6.81 (d, *J* = 8.8 Hz, 2H), 5.04 (s, 4H), 4.40 (m, 4H), 4.13 – 4.09 (m, 2H), 3.93 (dd, *J* = 9.0, 7.0 Hz, 2H), 3.12 (m, 4H), 1.98 (m, 8H), 0.95 – 0.80 (m, 24H).

^{13}C NMR (125 MHz, DMSO) δ 172.55, 171.53, 171.37, 163.34, 156.55, 147.15, 139.84, 137.53, 133.07, 132.37, 128.77, 128.20, 128.08, 128.04, 127.95, 124.04, 119.76, 119.64, 117.11, 116.45, 65.82, 60.78, 58.41, 47.58, 36.16, 30.98, 30.67, 30.26, 19.68, 18.84, 18.63.

HRMS-MALDI+ *calc* for [M+Na^+]: 1313.5209; found: 1313.5223

4.5 NMR Spectra

^{1}H NMR (300 MHz, $CDCl_3$) of compound **4**

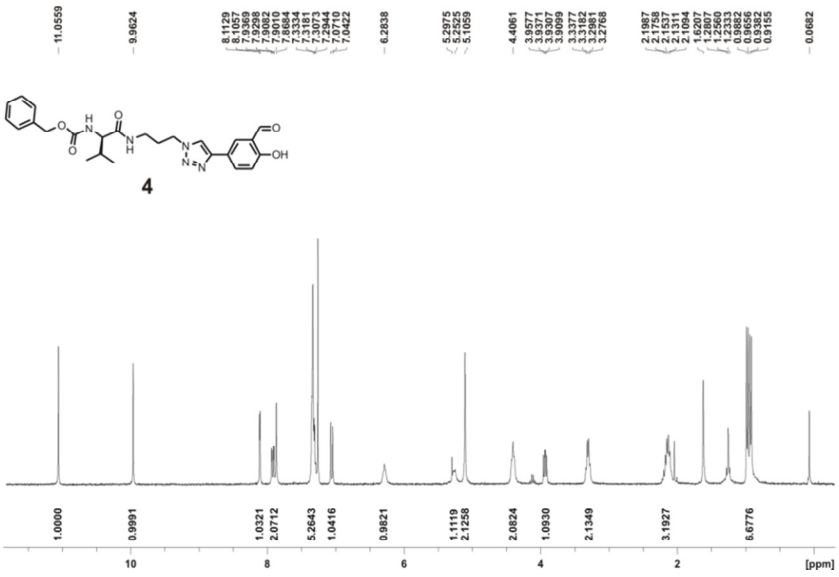

^{13}C NMR (125 MHz, $CDCl_3$) of compound **4**

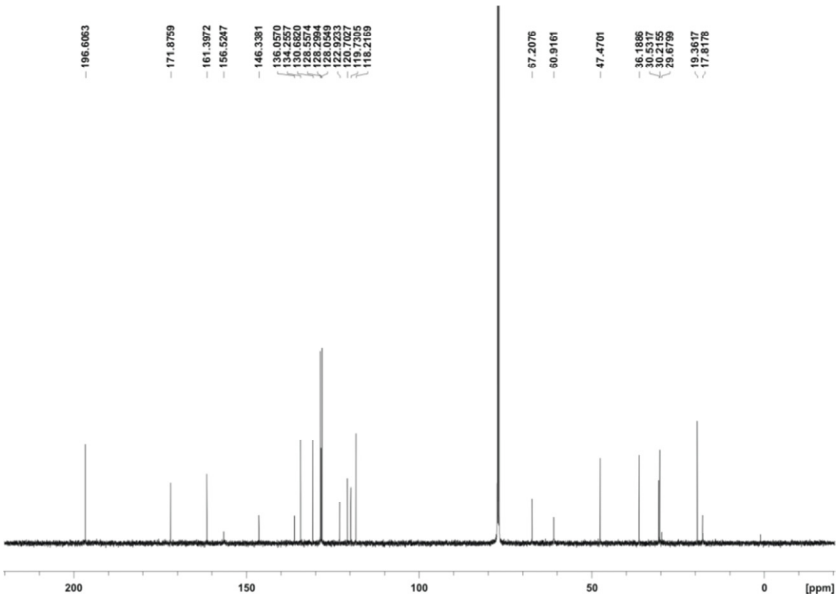

^{1}H NMR (500 MHz, DMSO-d_6) of compound **1a**

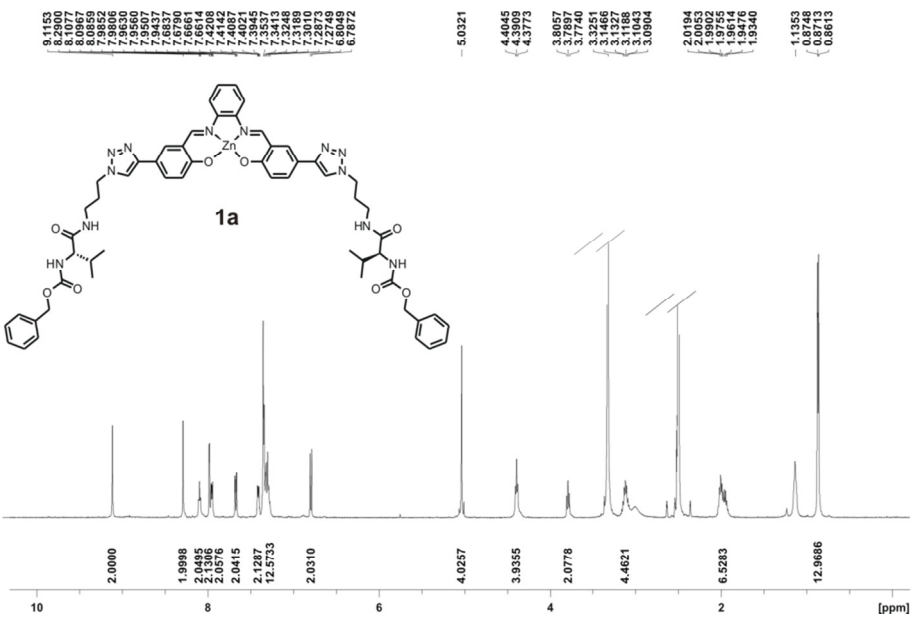

^{13}C NMR (125 MHz, DMSO) of compound **1a**

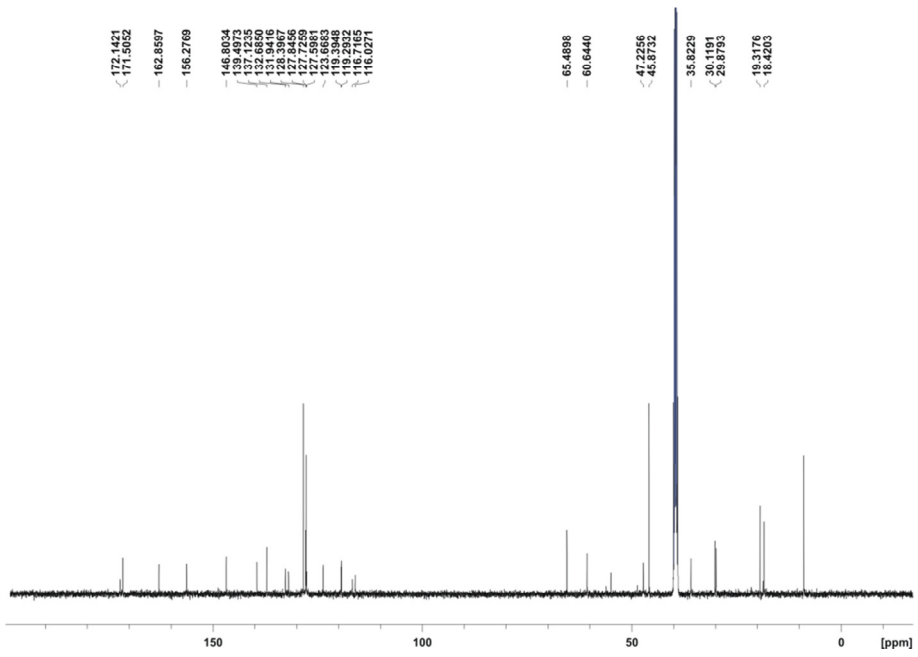

^{1}H NMR (400 MHz, $CDCl_3$) of compound **5**

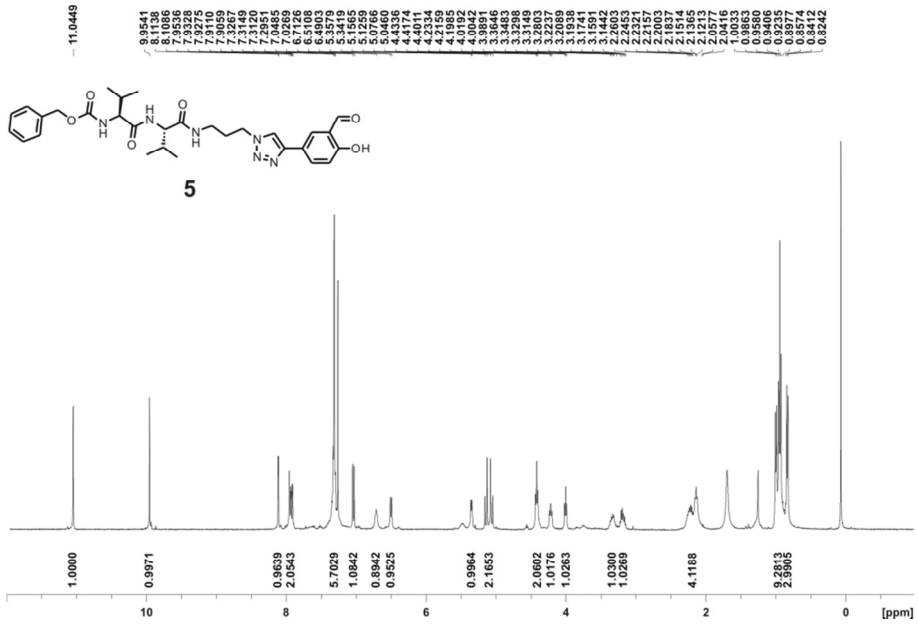

^{13}C NMR (126 MHz, $CDCl_3$) of compound **5**

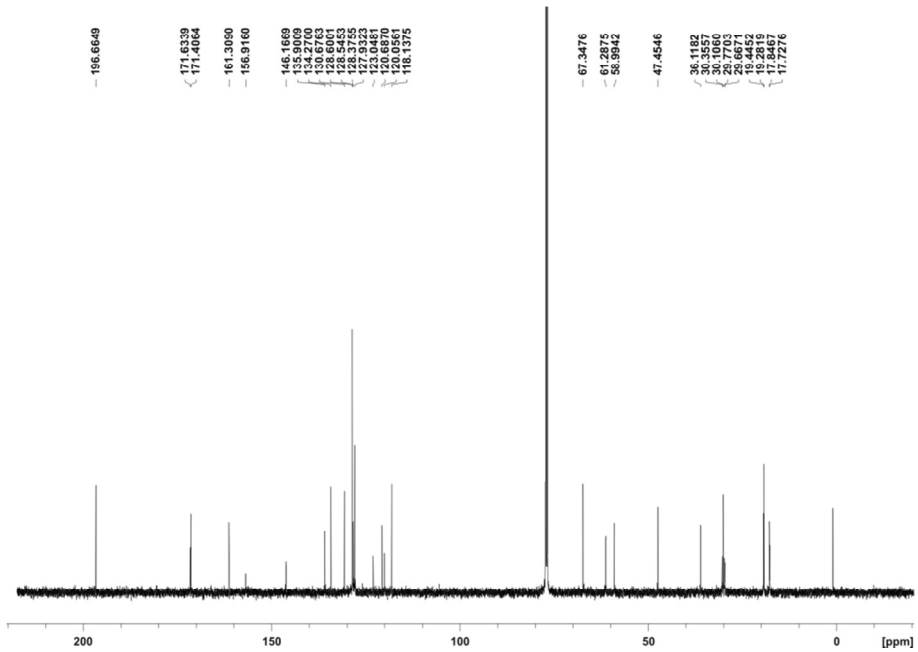

^{1}H NMR (500 MHz, DMSO-d_6) of compound **1b**

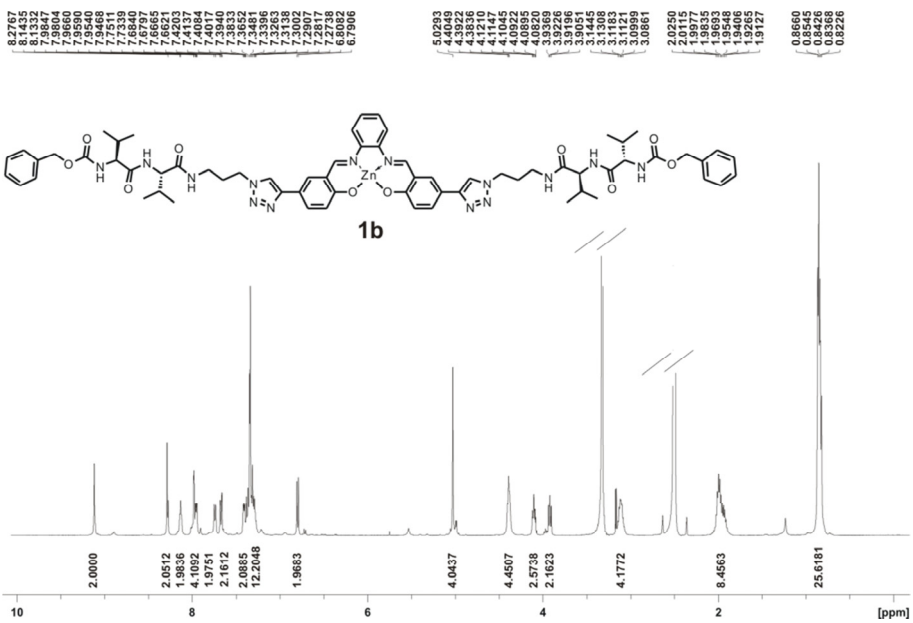

^{13}C NMR (125 MHz, DMSO) of compound **1b**

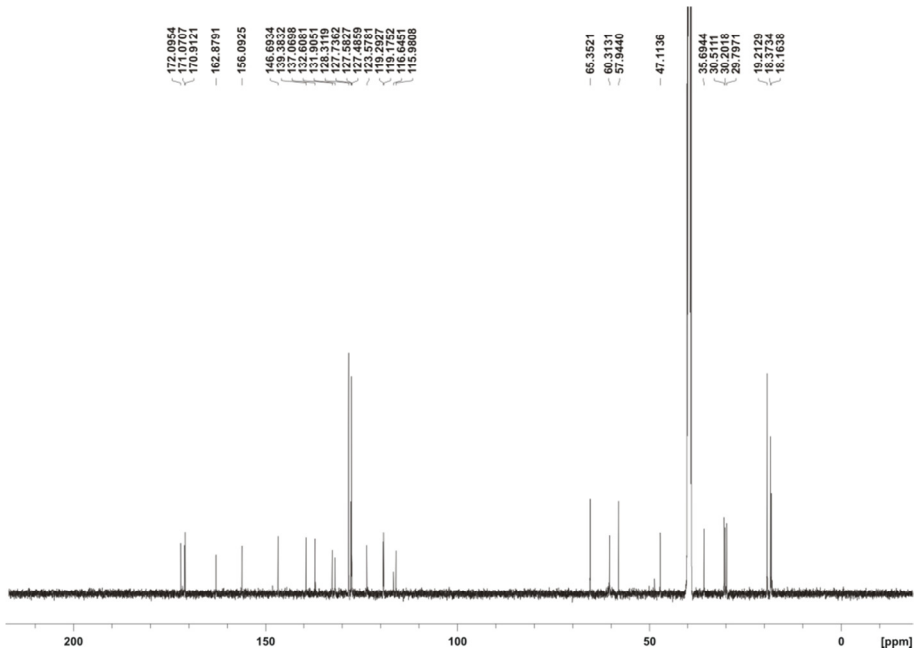

4.6 References

[1] Lloyd, D. Jordan, *Colloid chemistry* **1926**, *1*, 767-782
[2] M. D. Segarra-Maset, V. J. Nebot, J. F. Miravet, B. Escuder, *Chem. Soc. Rev.* **2013**, *42*, 7086-7098.
[3] J. W. Steed, *Chem. Commun.* **2011**, *47*, 1379-1383.
[4] D. J. Abdallah, R. G. Weiss, *Advanced Materials* **2000**, *12*, 1237-1247.
[5] J. H. van Esch, B. L. Feringa, *Angew. Chem., Int. Ed. Engl.* **2000**, *39*, 2263-2266.
[6] A. R. Hirst, I. A. Coates, T. R. Boucheteau, J. F. Miravet, B. Escuder, V. Castelletto, I. W. Hamley, D. K. Smith, *J. Am. Chem. Soc.* **2008**, *130*, 9113-9121.
[7] J. A. Foster, J. W. Steed, *Angew. Chem., Int. Ed. Engl.* **2010**, *49*, 6718-6724.
[8] V. J. Nebot, J. Armengol, J. Smets, S. F. Prieto, B. Escuder, J. F. Miravet, *Chem. Eur. J.* **2012**, *18*, 4063-4072.
[9] B. Escuder, F. Rodriguez-Llansola, J. F. Miravet, *New J. Chem.* **2010**, *34*, 1044-1054.
[10] A. R. Hirst, B. Escuder, J. F. Miravet, D. K. Smith, *Angew. Chem., Int. Ed. Engl.* **2008**, *47*, 8002-8018.
[11] J. F. Miravet, B. Escuder, *Tetrahedron* **2007**, *63*, 7321-7325.
[12] J. A. Foster, M. O. M. Piepenbrock, G. O. Lloyd, N. Clarke, J. A. K. Howard, J. W. Steed, *Nat. Chem.* **2010**, *2*, 1037-1043.
[13] H. Y. Li, Y. Fujiki, K. Sada, L. A. Estroff, *CrystEngComm* **2011**, *13*, 1060-1062.
[14] K. Tiefenbacher, H. Dube, D. Ajami, J. Rebek, *Chem. Commun.* **2011**, *47*, 7341-7343.
[15] F. Fages, *Angew. Chem., Int. Ed. Engl.* **2006**, *45*, 1680-1682.
[16] J. A. Saez, B. Escuder, J. F. Miravet, *Chem. Commun.* **2010**, *46*, 7996-7998.
[17] M. O. M. Piepenbrock, G. O. Lloyd, N. Clarke, J. W. Steed, *Chemical Reviews* **2010**, *110*, 1960-2004.
[18] B. Verdejo, F. Rodriguez-Llansola, B. Escuder, J. F. Miravet, P. Ballester, *Chem. Commun.* **2011**, *47*, 2017-2019.
[19] K. Q. Fan, J. Song, J. J. Li, X. D. Guan, N. M. Tao, C. Q. Tong, H. H. Shen, L. B. Niu, *J. Mater. Chem. C* **2013**, *1*, 7479-7482.
[20] H. Maeda, *Chem. Eur. J.* **2008**, *14*, 11274-11282.
[21] G. O. Lloyd, J. W. Steed, *Nat. Chem.* **2009**, *1*, 437-442.
[22] A. Dalla Cort, P. De Bernardin, G. Forte, F. Y. Mihan, *Chem. Soc. Rev.* **2010**, *39*, 3863-3874.
[23] A. W. Kleij, M. Kuil, M. Lutz, D. M. Tooke, A. L. Spek, P. C. J. Kamer, P. W. N. M. van Leeuwen, J. N. H. Reek, *Inorg. Chim. Acta* **2006**, *359*, 1807-1814.
[24] J. K. H. Hui, Z. Yu, M. J. MacLachlan, *Angew. Chem., Int. Ed. Engl.* **2007**, *46*, 7980-7983.
[25] J. K. H. Hui, Z. Yu, T. Mirfakhrai, M. J. MacLachlan, *Chem. Eur. J.* **2009**, *15*, 13456-13465.
[26] I. P. Oliveri, S. Failla, G. Malandrino, S. Di Bella, *J. Phys. Chem. C* **2013**, *117*, 15335-15341.
[27] I. P. Oliveri, G. Malandrino, S. Di Bella, *Dalton Trans.* **2014**, *43*, 10208-10214.
[28] B. Escuder, J. F. Miravet, *Langmuir* **2006**, *22*, 7793-7797.
[29] V. J. Nebot, J. Armengol, J. Smets, S. F. Prieto, B. Escuder, J. F. Miravet, *Chem. Eur. J.* **2012**, *18*, 4063-4072.

[30] A. R. Hirst, I. A. Coates, T. R. Boucheteau, J. F. Miravet, B. Escuder, V. Castelletto, I. W. Hamley, D. K. Smith, *J. Am. Chem. Soc.* **2008**, *130*, 9113-9121.